Synthesis of a Series of Octabutoxy- and Octabutoxybenzophthalocyanines and Photophysical Properties of Two Members of the Series

Mohamed Aoudia,[†] Gongzhen Cheng,[‡] Vance O. Kennedy,[‡] Malcolm E. Kenney,*[,‡] and Michael A. J. Rodgers*[,†]

Contribution from the Center for Photochemical Sciences, Bowling Green State University, Bowling Green, Ohio 43403, and Department of Chemistry, Case Western Reserve University, Cleveland, Ohio 44106

Received October 23, 1996[⊗]

Abstract: We have developed a new route to silicon-centered phthalocyanines and phthalocyanine-like compounds that is robust and flexible, and of considerable potential usefulness. This route entails insertion of silicon into the metal-free macrocycle. It has been developed in the course of preparing four new and two known metal-free, six new dihydroxysilicon, and six new bis-trihexylsiloxysilicon octabutoxy- and octabutoxybenzophthalocyanines. One of the siloxysilicon compounds, that with the ligand 5,9,12,16,19,23,28,32-octabutoxy-33*H*,35*H*-dibenzo[*b*,*g*]dinaphtho-[2,3-*l*:2′,3′-*q*]porphyrazine, has a Q-band at a wavelength of 804 nm and an extinction coefficient of 1.9×10^5 M^{-1} cm^{-1}. Its wavelength thus matches the wavelength of the output of the most common GaAlAs diode laser. The compound and its analog in which the benzo rings are *trans* to each other instead of *cis* have no tendency to aggregate in benzene up to a concentration of 150 μM. The triplet state of the *cis* isomer has an absorption maximum at 640 nm and a lifetime in deaerated benzene solution of 105 μs, while the triplet state of the *trans* isomer has a maximum at 660 nm and a lifetime of 72 μs. Both isomers have a triplet quantum yield, Q_t, of *ca*. 0.20 and a singlet oxygen quantum yield, Q_Δ, of *ca*. 0.20, photochemical properties that are consistent with potentially efficient photosensitization action in photodynamic therapy of tumors. For both sensitizers, energy transfer from the sensitizer triplet to ground state of dioxygen is reversible at appropriate concentrations. For the *cis* isomer, the equilibrium constant for the energy transfer process, K_e, is 0.012 ± 0.001, and the triplet state energy calculated from this, E_T, is 21.29 kcal/mol (E_T derived from phosphorescence measurements is 21.26 kcal/mol). For the *trans* isomer, K_e is 3.68×10^{-3} and E_T is 19.27 kcal/mol.

Introduction

In recent years significant research activity has been expended on phthalocyanine and phthalocyanine-like compounds that absorb strongly in the red or near-infrared regions.[1] Much of this effort has been concerned with the synthesis of these compounds and with an examination of their ground state and excited state photophysical properties. In part, the driving force for this synthetic and photophysical work stems from an intrinsic curiosity about how such compounds can be made and about the properties of low-lying electronic states. In addition, it derives from the potential which some of these compounds have for use as photosensitizers in photodynamic therapy (PDT)[2,3] and as red or near-infrared light absorbers in optical data storage systems.[4]

In our laboratories and in a few others, a focus has been on the synthesis of phthalocyanines and naphthalocyanines having potential for use in PDT and on evaluation of the photosensitizing efficacy and phototherapeutic capability of the compounds prepared.[5−25] Most of the compounds prepared have Q-bands with extinction coefficients of *ca*. 10^5 M^{-1} cm^{-1} and absorption maxima in the range of 670−900 nm, the values of the maxima depending critically on the type of substitution present, if any, on the tetrapyrrolic π-system and on the nature of the central

* Authors to whom correspondence should be addressed at the following: M.A.J.R. phone 419-372-7606; fax 419-372-9300; e-mail rodgers@bgnet.bgsu.edu. M.E.K. phone 216-368-3739; fax 216-368-3006; e-mail mek9@po.cwru.edu

† Bowling Green State University.

‡ Case Western Reserve University.

⊗ Abstract published in *Advance ACS Abstracts*, June 1, 1997.

(1) *Infrared Absorbing Dyes*; Matsuoka, M., Ed.; Plenum: New York, 1990, and references therein.

(2) Kessel, D. *Spectrum* **1990**, *3* (4), 13.

(3) Spikes, J. D. *Photochem. Photobiol.* **1986**, *43*, 691.

(4) Matsui, F. In *Infrared Absorbing Dyes*; Matsuoka, M., Ed.; Plenum: New York, 1990; Chapter 10.

(5) Firey, P. A.; Ford, W. E.; Sounik, J. R.; Kenney, M. E.; Rodgers, M. A. J. *J. Am. Chem. Soc.* **1988**, *110*, 7626.

(6) Rihter, B. D.; Kenney, M. E.; Ford, W. E.; Rodgers, M. A. J. *J. Am. Chem. Soc.* **1990**, *112*, 8064.

(7) Rihter, B. D.; Bohorquez, M. D.; Rodgers, M. A. J.; Kenney, M. E. *Photochem. Photobiol.* **1992**, *55*, 677.

(8) Ford, W. E.; Rodgers, M. A. J.; Schechtman, L. A.; Sounik, J. R.; Rihter, B. D.; Kenney, M. E. *Inorg. Chem.* **1992**, *31*, 3371.

(9) Rihter, B. D.; Kenney, M. E.; Ford, W. E.; Rodgers, M. A. J. *J. Am. Chem. Soc.* **1993**, *115*, 8146.

(10) Cuomo, V.; Jori, G.; Rihter, B.; Kenney, M. E.; Rodgers, M. A. J. *Br. J. Cancer* **1991**, *64*, 93.

(11) Bellemo, C.; Jori, G.; Rihter, B. D.; Kenney, M. E.; Rodgers, M. A. J. *Cancer Lett.* **1992**, *65*, 145.

(12) Zuk, M. M.; Rihter, B. D.; Kenney, M. E.; Rodgers, M. A. J.; Kreimer-Birnbaum, M. *Photochem. Photobiol.* **1994**, *59*, 66.

(13) Biolo, R.; Jori, G.; Soncin, M.; Pratesi, R.; Vanni, U.; Rihter, B. D.; Kenney, M. E.; Rodgers, M. A. J. *Photochem. Photobiol.* **1994**, *59*, 362.

(14) Soncin, M.; Polo, L.; Reddi, E.; Jori, G.; Kenney, M. E.; Cheng, G.; Rodgers, M. A. J. *Cancer Lett.* **1995**, *89*, 101.

(15) Soncin, M.; Polo, L.; Reddi, E.; Jori, G.; Rihter, B. D.; Kenney, M. E.; Rodgers, M. A. J. *Photochem. Photobiol.* **1995**, *61*, 310.

(16) van Lier, J. E. In *Photodynamic Therapy of Neoplastic Disease*; Kessel, D., Ed.; CRC Press: Boca Raton, FL, 1990; p 279.

(17) Rosenthal, I. *Photochem. Photobiol.* **1991**, *53*, 859.

(18) Wagner, J. R.; Ali, H.; Langlois, R.; Brassma, N.; van Lier, J. E. *Photochem. Photobiol.* **1987**, *45*, 587.

(19) Dhami, S.; DeMello, A. J.; Rumbles, G.; Bishop, S. M.; Phillips, D.; Beeby, A. *Photochem. Photobiol.* **1995**, *61*, 341.

(20) Brasseur, N.; Ali, H.; Langlois, R.; Vagner, R.; Rousseau, J.; van Lier, J. E. *Photochem. Photobiol.* **1987**, *45*, 581.

(21) Ben-Hur, E.; Rosenthal, I. *Photochem. Photobiol.* **1986**, *43*, 129.

(22) Berg, K.; Bommer, J. C.; Moan, J. *Cancer Lett.* **1989**, *44*, 7.

S0002-7863(96)03702-X CCC: $14.00

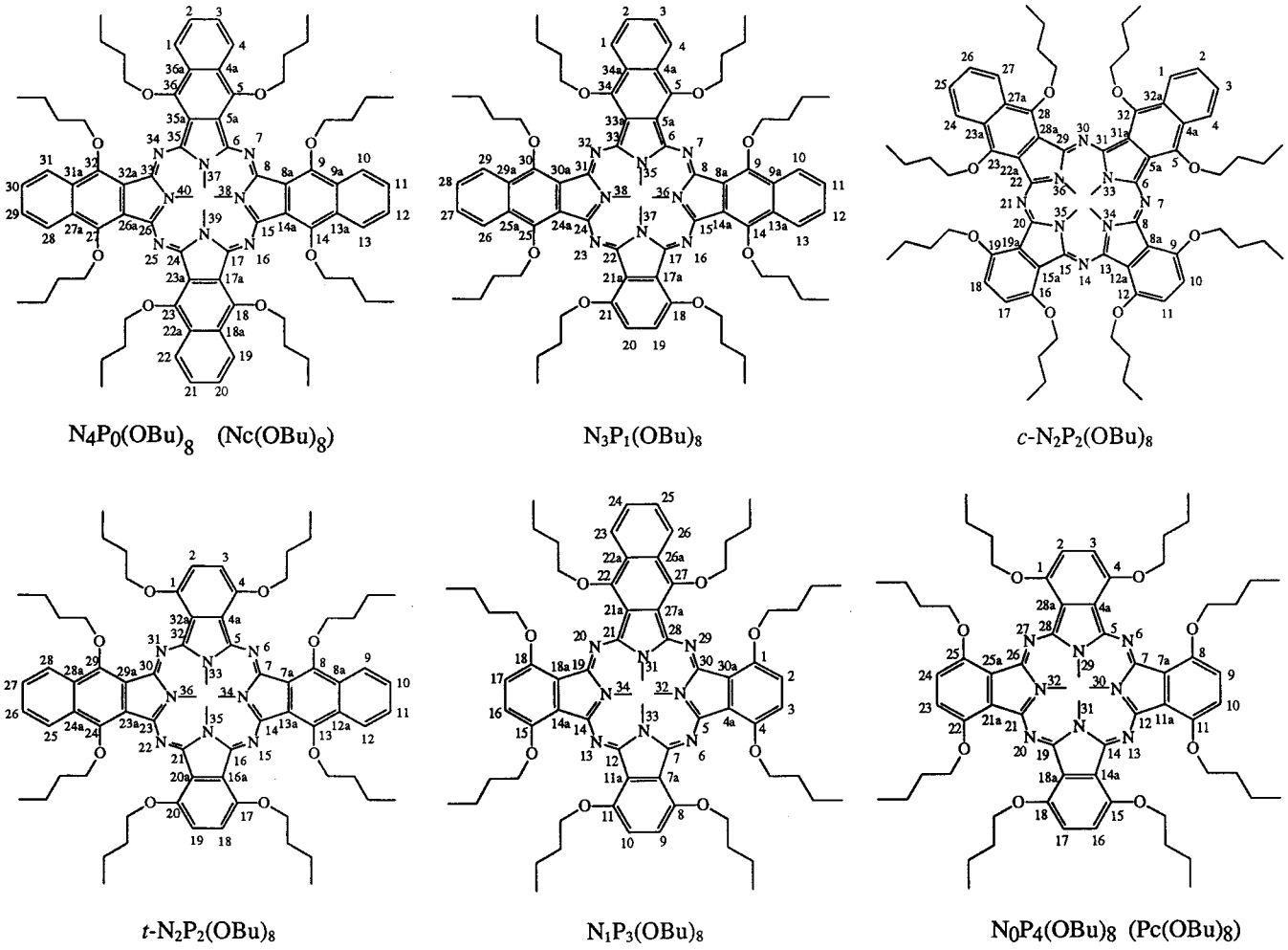

Figure 1. Structures and numbering schemes of the ring systems.

metal atom. Many of the compounds of this type are very stable, can be synthesized in high purity in useful amounts (>100 mg), and possess photophysical properties appropriate to their use in PDT.[3,5−17] On the negative side, many of them are highly lipophilic, a characteristic which can cause them to aggregate in solution.[18,19] This is of considerable importance because the aggregation of photosensitizers often affects their excited states in such a way as to reduce their photosensitizing activity. However, it has been shown that the tendency of phthalocyanines and naphthalocyanines to aggregate can be reduced by substituting appropriate groups, for example, sulfonic acid groups[20−24] or dibenzobarreleno groups,[7] on their rings.

In this study, the synthesis of three series of hindered phthalocyanines is described. One series is composed of metal-free octabutoxy- and octabutoxybenzophthalocyanines, the second of their dihydroxysilicon analogs, and the third of their bis-trihexylsiloxysilicon analogs. All of the compounds in these three series, with the exception of the end members of the first,[26] are new. These three series were prepared in an attempt to gain insight into the relationship between ring structure and Q-band position in the series and, in addition, to try to find a compound having a Q-band in the 805 nm region. This particular wavelength region is of interest because it is the region that is most readily available from the highly reliable and inexpensive, and thus phototherapeutically desirable, GaAlAs diode laser.

We found that the relationship between structure and Q-band position is understandable and that the bis-trihexylsilicon compound with the *c*-$N_2P_2(OBu)_8$ ring (Figure 1), that is, *c*-$SiN_2P_2(OBu)_8(OSi(n\text{-}C_6H_{13})_3)_2$, has a Q-band at 804 nm. Having found a compound with the desired Q-band, we then investigated its photophysical characteristics and those of its isomer, *t*-$SiN_2P_2(OBu)_8(OSi(n\text{-}C_6H_{13})_3)_2$. The results of this work are described and discussed.

Experimental Section

(A) Synthesis.[27] **$H_2N_{4-x}P_x(OBu)_8$.** Under Ar, a mixture of 3,6-dibutoxy-1,2-benzenedicarbonitrile (279 mg, 1.00 mmol, available from Aldrich Chemical Co., Milwaukee, WI), 1,4-dibutoxy-2,3-naphthalenedicarbonitrile (326 mg, 1.00 mmol, available from Aldrich), and 1-butanol (22 mL) was brought to reflux, treated with Li shot (pentane washed, 450 mg, 65.0 mmol), refluxed for 1 h, and cooled. The resulting solution was stirred with H_2O (25 mL, 1.4 mol) for 2.5 h, and the hydrolysate obtained was extracted with toluene (*i.e.*, repeatedly stirred with toluene) (5 times, 50 mL each time). The extracts were combined, filtered, and evaporated to dryness with a rotary evaporator (60 °C, ~30 Torr), and the solid was extracted with toluene (50 mL). The extract was evaporated to dryness with a rotary evaporator (60 °C, ~30 Torr) (600 mg).

The product is a greenish-brown solid. It is soluble in toluene, CH_2Cl_2, and pyridine and slightly soluble in hexane.

$H_2N_4P_0(OBu)_8$ ($H_2Nc(OBu)_8$).[26] $H_2N_{4-x}P_x(OBu)_8$ (600 mg) was chromatographed (wet loading, hexane; Al_2O_3 III, hexane, 1.5 × 20 cm; hexane; filtration; rotary evaporation (45 °C, ~20 Torr)). The solid isolated was washed with pentane (5 mL), dried (~60 °C, ~25

(23) Peng, Q.; Moan, J.; Nesland, J. M.; Rimington, C. *Int. J. Cancer* **1990**, *46*, 719.

(24) Tralau, C. T.; MacRobert, A. J.; Coleridge-Smith, P. D.; Barr, H.; Bown, S. G. *Br. J. Cancer* **1987**, *55*, 389.

(25) Kreimer-Birnbaum, M. *Semin. Hematol*. **1989**, *26*, 157.

(26) Cook, M. J.; Dunn, A. J.; Howe, S. D.; Thomson, A. J.; Harrison, K. J. *J. Chem. Soc., Perkin Trans. 1* **1988**, 2453.

(27) Abbreviations: Nc, naphthalocyanine; Pc, phthalocyanine; $H_2N_{4-x}P_x(OBu)_8$, series of six macrocycles with the ring systems shown in Figure 1.

Torr), and weighed (5 mg, 1% of weight of $H_2N_{4-x}P_x(OBu)_8$). UV−vis (λ_{max} (nm), ϵ (M^{-1} cm^{-1})) (toluene, 2.1 mM): 862, 2.0×10^5. ^{1}H NMR (C_6D_6): δ 9.23 (m, 1,4,10,13,19,22,28,31-Ar H), 7.68 (m, 2,3,-11,12,20,21,29,30-Ar H), 5.40 (t, OR-1 CH_2), 2.38 (m, OR-2 CH_2), 2.27 (s, NH), 1.67 (m, OR-3 CH_2), 1.03 (t, OR CH_3). ^{13}C NMR (C_6D_6): δ 150.59 (5,9,14,18,23,27,32,36-Ar C; 6,8,15,17,24,26,33,35-Ar C), 131.54 (4a,9a,13a,18a,22a,27a,31a,36a-Ar C), 127.60 (2,3,11,-12,20,21,29,30-Ar C), 124.91 (1,4,10,13,19,22,28,31-Ar C), 123.51 (5a,8a,14a,17a,23a,26a,32a,35a-Ar C), 77.24 (OR-1 C), 33.34 (OR-2 C), 20.07 (OR-3 C), 14.49 (OR-4 C).

The compound is a brown solid. It is soluble in toluene, CH_2Cl_2, and pyridine and slightly soluble in hexane.

$H_2N_3P_1(OBu)_8$. The chromatography of the $H_2N_{4-x}P_x(OBu)_8$ was continued (toluene). The fraction isolated was treated in the same way as the first one (34 mg, 6% of weight of $H_2N_{4-x}P_x(OBu)_8$). UV−vis (λ_{max} (nm), ϵ (M^{-1} cm^{-1})) (toluene, 1.9 μM): 814, 0.99×10^5; 851, 0.89×10^5. ^{1}H NMR (C_6D_6): δ 9.23 (m, 1,4-Ar H; 10,29-Ar H; 13,-26-Ar H), 7.69 (m, 2,3-Ar H; 11,28-Ar H; 12,27-Ar H), 7.44 (s, 19,-20-Ar H), 5.55 (t, 5,34-OR-1 CH_2), 5.39 (t, 9,30-OR-1 CH_2), 5.31 (t, 14,25-OR-1 CH_2), 4.75 (t, 18,21-OR-1 CH_2), 2.34 (m, 5,34-OR-2 CH_2; 9,30-OR-2 CH_2), 2.24 (m, 14,25-OR-2 CH_2; 18,21-OR-2 CH_2), 1.91 (s, NH), 1.85 (m, 5,34-OR-3 CH_2; 9,30-OR-3 CH_2), 1.66 (m, 14,25-OR-3 CH_2; 18,21-OR-3 CH_2), 1.13 (t, 5,34-OR CH_3), 1.02 (m, 9,30-OR CH_3; 14,25-OR CH_3), 0.96 (t, 18,21-OR CH_3). ^{13}C NMR (C_6D_6): δ 152.22 (17,22-Ar C), 151.50 (18,21-Ar C), 150.63 (5,34-Ar C; 6,-33-Ar C), 149.99 (8,31-Ar C; 9,30-Ar C; 14,25-Ar C; 15,24-Ar C), 131.97 (4a,34a-Ar C), 131.67 (9a,29a-Ar C; 13a,25a-Ar C), 127.73 (17a,21a-Ar C), 127.53 (2,3-Ar C), 127.41 (11,28-Ar C; 12,27-Ar C), 125.69 (1,4-Ar C), 124.91 (10,29-Ar C; 13,26-Ar C), 121.42 (5a,33a-Ar C; 8a,30a-Ar C; 14a,24a-Ar C), 117.28 (19,20-Ar C), 77.35 (5,34-OR-1 C; 9,30-OR-1 C), 77.27 (14,25-OR-1 C), 72.23 (18,21-OR-1 C), 33.67 (5,34-OR-2 C), 33.31 (9,30-OR-2 C; 14,25-OR-2 C), 32.37 (18,-21-OR-2 C), 20.33 (5,34-OR-3 C), 20.12 (9,30-OR-3 C; 14,25-OR-3 C), 20.03 (18,21-OR-3 C), 14.46 (5,34-OR-4 C; 9,30-OR-4 C; 14,25-OR-4 C; 18,21-OR-4 C). MS-HRFAB exact mass, *m*/*z*: calcd for $C_{76}H_{88}N_8O_8$ $(M + H)^+$, 1241.6803; found, 1241.6807, 1241.6795.

The compound is a brown solid. It is soluble in toluene, CH_2Cl_2, and pyridine and slightly soluble in hexane.

***c*-$H_2N_2P_2(OBu)_8$.** The chromatography of the $H_2N_{4-x}P_x(OBu)_8$ was continued further (toluene/CH_2Cl_2, 1:1). The fraction separated was treated in the same way as the previous two fractions (62 mg, 10% of weight of $H_2N_{4-x}P_x(OBu)_8$). UV−vis (λ_{max} (nm), ϵ (M^{-1} cm^{-1})) (toluene, 2.2 μM): 807, 1.9×10^5. ^{1}H NMR (C_6D_6): δ 9.21 (m, 1,-27-Ar H; 4,24-Ar H), 7.67 (m, 2,26-Ar H; 3,25-Ar H), 7.52 (d, 10,-18-Ar H), 7.40 (d, 11,17-Ar H), 5.51 (t, 28,32-OR-1 CH_2), 5.30 (t, 5,23-OR-1 CH_2), 4.95 (t, 9,19-OR-1 CH_2), 4.71 (t, 12,16-OR-1 CH_2), 2.31 (m, 5,23-OR-2 CH_2; 28,32-OR-2 CH_2), 2.20 (m, 9,19-OR-2 CH_2; 12,16-OR-2 CH_2), 1.80 (m, 5,23-OR-3 CH_2; 28,32-OR-3 CH_2), 1.62 (m, 9,19-OR-3 CH_2; 12,16-OR-3 CH_2), 1.54 (s, NH), 1.10 (t, 28,32-OR CH_3), 1.06 (t, 5,23-OR CH_3), 1.00 (t, 9,19-OR CH_3), 0.94 (t, 12,-16-OR CH_3). ^{13}C NMR (C_6D_6): δ 152.38 (13,15-Ar C), 152.20 (8,20-Ar C; 9,19-Ar C; 12,16-Ar C), 150.70 (6,22-Ar C; 29,31-Ar C), 150.33 (5,23-Ar C; 28,32-Ar C), 131.98 (27a,32a-Ar C), 131.21 (4a,23a-Ar C), 126.85 (8a,19a-Ar C; 12a,15a-Ar C), 127.75 (2,26-Ar C; 3,25-Ar C), 125.01 (1,27-Ar C), 124.92 (4,24-Ar C), 123.71 (5a,22a-Ar C), 123.11 (28a,31a-Ar C), 119.89 (10,18-Ar C), 117.59 (11,17-Ar C), 77.50 (28,32-OR-1 C), 77.29 (5,23-OR-1 C), 72.98 (9,19-OR-1 C), 72.16 (12,16-OR-1 C), 33.61 (28,32-OR-2 C), 33.29 (5,23-OR-2 C), 32.53 (9,19-OR-2 C), 32.38 (12,16-OR-2 C), 20.09 (5,23-OR-3 C; 28,-32-OR-3 C), 20.01 (9,19-OR-3 C; 12,16-OR-3 C), 14.44 (5,23-OR-4 C; 9,19-OR-4 C; 12,16-OR-4-C; 28,32-OR-4 C). MS-HRFAB exact mass, *m*/*z*: calcd for $C_{72}H_{86}N_8O_8$ $(M + H)^+$, 1191.6647; found, 1191.6677, 1191.6598.

The compound is a dark-green solid. It is soluble in toluene, CH_2Cl_2, and pyridine and slightly soluble in hexane.

***t*-$H_2N_2P_2(OBu)_8$.** The chromatography of the $H_2N_{4-x}P_x(OBu)_8$ was continued still further (CH_2Cl_2), and the resulting fraction was treated as before (12 mg, 2% of weight of $H_2N_{4-x}P_x(OBu)_8$). UV−vis (λ_{max} (nm), ϵ (M^{-1} cm^{-1})) (toluene, 1.7 μM): 750, 0.98×10^5; 852, 0.75×10^5. ^{1}H NMR (C_6D_6): δ 9.23 (m, 9,12,25,28-Ar H), 7.69 (m, 10,11,-26,27-Ar H), 7.47 (s, 2,3,18,19-Ar H), 5.48 (t, 8,13,24,29-OR-1 CH_2), 4.75 (t, 1,4,17,20-OR-1 CH_2), 2.32 (m, 8,13,24,29-OR-2 CH_2), 2.22 (m, 1,4,17,20-OR-2 CH_2), 1.83 (m, 8,13,24,29-OR-3 CH_2), 1.60 (m, 1,4,17,20-OR-3 CH_2), 1.11 (t, 8,13,24,29-OR CH_3), 0.95 (t, 1,4,17,-20-OR CH_3). ^{13}C NMR (C_6D_6): δ 152.20 (1,4,17,20-Ar C; 5,16,20,-32-Ar C), 150.72 (7,14,23,30-Ar C; 8,13,24,29-Ar C), 131.89 (8a,-12a,24a,28a-Ar C), 127.36 (10,11,26,27-Ar C), 127.17 (4a,16a,20a,32a-Ar C), 126.15 (7a,13a,23a,29a-Ar C), 125.02 (9,12,25,28-Ar C), 118.32 (2,3,18,19-Ar C), 77.42 (8,13,24,29-OR-1 C), 72.37 (1,4,17,20-OR-1 C), 33.65 (8,13,24,29-OR-2 C), 32.35 (1,4,17,20-OR-2 C), 20.10 (1,4,-17,20-OR-3 C; 8,13,24,29-OR-3 C), 14.46 (1,4,17,20-OR-4 C; 8,13,-24,29-OR-4 C). MS-HRFAB exact mass, *m*/*z*: calcd for $C_{72}H_{86}N_8O_8$ $(M + H)^+$, 1191.6647; found, 1191.6632, 1191.6592.

The compound is a brown solid. It is soluble in toluene, CH_2Cl_2, and pyridine and slightly soluble in hexane.

$H_2N_1P_3(OBu)_8$. The chromatography of the $H_2N_{4-x}P_x(OBu)_8$ was continued further yet (toluene/ethyl acetate, 1:1), and the fraction isolated was treated as before (102 mg, 17% of weight of $H_2N_{4-x}P_x(OBu)_8$). UV−vis (λ_{max} (nm), ϵ (M^{-1} cm^{-1})) (toluene, 1.5 μM): 756, 0.82×10^5; 802, 0.66×10^5. ^{1}H NMR (C_6D_6): δ 9.22 (m, 23,26-Ar H), 7.68 (m, 24,25-Ar H), 7.56 (d, 2,17-Ar H), 7.51 (s, 9,-10-Ar H), 7.43 (d, 3,16-Ar H), 5.45 (t, 22,27-OR-1 CH_2), 4.94 (m, 1,18-OR-1 CH_2; 4,15-OR-1 CH_2), 4.70 (t, 8,11-OR-1 CH_2), 2.30 (m, 22,27-OR-2 CH_2), 2.21 (m, 1,18-OR-2 CH_2; 4,15-OR-2 CH_2; 8,11-OR-2 CH_2), 1.78 (m, 22,27-OR-3 CH_2), 1.75 (m, 1,18-OR-3 CH_2; 4,-15-OR-3 CH_2; 8,11-OR-3 CH_2), 1.18 (t, 22,27-OR CH_3), 1.13 (t, 1,18-OR CH_3; 4,15-OR CH_3), 0.93 (t, 8,11-OR CH_3), 0.63 (s, NH). ^{13}C NMR (C_6D_6): δ 152.62 (21,28-Ar C), 152.41 (1,18-Ar C; 4,15-Ar C; 5,14-Ar C; 7,12-Ar C; 8,11-Ar C; 19,30-Ar C), 150.73 (22,27-Ar C), 132.02 (22a,26a-Ar C), 129.84 (7a,11a-Ar C), 127.35 (24,25-Ar C), 126.04 (21a,27a-Ar C), 125.30 (4a,14a-Ar C; 18a,30a-Ar C), 125.05 (23,26-Ar C), 120.36 (2,17-Ar C), 120.05 (3,16-Ar C), 118.05 (9,10-Ar C), 77.50 (22,27-OR-1 C), 73.00 (1,18-OR-1 C; 4,15-OR-1 C), 72.22 (8,11-OR-1 C), 33.63 (22,27-OR-2 C), 32.57 (1,18-OR-2 C), 32.47 (4,15-OR-2 C), 32.35 (8,11-OR-2 C), 20.07 (1,18-OR-3 C; 22,27-OR-3 C), 19.99 (4,15-OR-3 C; 8,11-OR-3 C), 14.39 (1,18-OR-4 C; 4,15-OR-4 C; 8,11-OR-4 C; 22,27-OR-4 C). MS-HRFAB exact mass, *m*/*z*: calcd for $C_{68}H_{84}N_8O_8$ $(M + H)^+$, 1141.6490; found, 1141.6453, 1141.6449.

The compound is a dark-green solid. It is soluble in toluene, CH_2Cl_2, and pyridine and slightly soluble in hexane.

$H_2N_0P_4(OBu)_8$ ($H_2Pc(OBu)_8$).[26,28,29] The chromatography of the $H_2N_{4-x}P_x(OBu)_8$ was continued yet again (ethyl acetate), and the fraction separated was treated as before (30 mg, 5% of weight of $H_2N_{4-x}P_x(OBu)_8$). UV−vis (λ_{max} (nm), ϵ (M^{-1} cm^{-1})) (toluene, 2.1 μM): 739, 0.95×10^5; 761, 1.1×10^5. ^{1}H NMR (C_6D_6): δ 7.53 (s, Ar H), 4.91 (t, OR-1 CH_2), 2.20 (m, OR-2 CH_2), 1.72 (m, OR-3 CH_2), 1.04 (t, OR CH_3), −0.28 (s, NH). ^{13}C NMR (C_6D_6): δ 152.63 (5,7,-12,14,19,21,26,28-Ar C), 149.20 (1,4,8,11,15,18,22,25-Ar C), 127.75 (4a,7a,11a,14a,18a,21a,25a,28a-Ar C), 120.33 (2,3,9,10,16,17,23,24-Ar C), 73.01 (OR-1 C), 32.51 (OR-2 C), 19.98 (OR-3 C), 14.37 (OR-4 C).

The compound is a green solid. It is soluble in toluene, CH_2Cl_2, and pyridine and slightly soluble in hexane.

$SiN_4P_0(OBu)_8(OH)_2$ ($SiNc(OBu)_8(OH)_2$). $SiN_4P_0(OBu)_8(OH)_2$ was prepared by the same type of procedure used for the synthesis of *c*-$SiN_2P_2(OBu)_8(OH)_2$ (**route 1**, see below) (78%). UV-vis (λ_{max} (nm), toluene): 865. ^{1}H NMR (C_6D_6): δ 9.23 (m, 1,4,10,13,19,22,28,31-Ar H), 7.68 (m, 2,3,11,12,20,21,29,30-Ar H), 5.35 (t, OR-1 CH_2), 2.35 (m, OR-2 CH_2), 1.65 (m, OR-3 CH_2), 1.03 (t, OR CH_3), −3.79 (s, br, OH). ^{13}C NMR (C_6D_6): δ 150.98 (6,8,15,17,24,26,33,35-Ar C), 148.37 (5,9,14,18,23,27,32,36-Ar C), 131.63 (4a,9a,13a,18a,22a,27a,31a,36a-Ar C), 127.73 (2,3,11,12,20,21,29,30-Ar C), 124.84 (1,4,10,13,19,22,-28,31-Ar C), 122.71 (5a,8a,14a,17a,23a,26a,32a,35a-Ar C), 77.47 (OR-1 C), 33.40 (OR-2 C), 19.98 (OR-3 C), 14.48 (OR-4 C).

The compound is a brown solid. It is soluble in toluene, CH_2Cl_2, and pyridine, and slightly soluble in hexane. Its crystals are acicular.

$SiN_3P_1(OBu)_8(OH)_2$. $SiN_3P_1(OBu)_8(OH)_2$ was prepared by route 1 (56%). UV−vis (λ_{max} (nm), toluene): 825; 861. ^{1}H NMR (C_6D_6): δ 9.22 (m, 1,4-Ar H; 10,29-Ar H; 13,26-Ar H), 7.64 (m, 2,3-Ar H; 11,-28-Ar H; 12,27-Ar H), 7.45 (s, 19,20-Ar H), 5.54 (t, 5,34-OR-1 CH_2), 5.36 (t, 9,30-OR-1 CH_2), 5.30 (t, 14,25-OR-1 CH_2), 4.75 (t, 18,21-

(28) Ford, W. E.; Rihter, B. D.; Kenney, M. E.; Rodgers, M. A. J. *Photochem. Photobiol.* **1989**, *50*, 277.

(29) Rihter, B. D.; Kenney, M. E.; Ford, W. E.; Rodgers, M. A. J. *J. Am. Chem. Soc.* **1990**, *112*, 8064.

OR-1 CH_2), 2.31 (m, 5,34-OR-2 CH_2; 9,30-OR-2 CH_2), 2.28 (m, 14,-25-OR-2 CH_2; 18,21-OR-2 CH_2), 1.86 (m, 5,34-OR-3 CH_2; 9,30-OR-3 CH_2), 1.77 (m, 14,25-OR-3 CH_2; 18,21-OR-3 CH_2), 1.18 (t, 5,34-OR CH_3), 1.10 (m, 9,30-OR CH_3; 14,25-OR CH_3), 1.04 (t, 18,21-OR CH_3).

The compound is a brown solid. It is soluble in toluene, CH_2Cl_2, and pyridine, and slightly soluble in hexane.

***c*-$SiN_2P_2(OBu)_8(OH)_2$.** Under Ar, $HSiCl_3$ (0.20 mL, 2.0 mmol) and a mixture of tributylamine (5.0 mL, 21 mmol), benzene (30 mL), and *c*-$H_2N_2P_2(OBu)_8$ (30 mg, 0.40 mmol), which had been dried by distillation (∼5 mL of distillate) were stirred for 24 h. More $HSiCl_3$ (0.20 mL, 2.0 mmol) was added, and the mixture was stirred for a further 24 h, and then still more $HSiCl_3$ (0.10 mL, 1.0 mmol) was added, and the mixture was stirred for an additional 72 h. The resultant mixture was mixed with H_2O (20 mL, 1.1 mmol), and the hydrolysate was mixed with triethylamine (10 mL, 99 mmol). The mixture formed was repeatedly extracted with toluene (5 times, 40 mL each time), and the extracts were combined, filtered, and evaporated to dryness with a rotary evaporator (80 °C). The solid was chromatographed (wet loading, toluene; Al_2O_3 III, toluene, 1.5 × 20 cm; toluene/ethyl acetate; filtration; rotary evaporation (45 °C, ∼ 5 Torr)), dried (70 °C, ∼25 Torr), and weighed (15 mg, 47%). UV−vis (λ_{max} (nm), toluene): 805. ^{1}H NMR (C_6D_6): δ 9.19 (m, 1,27-Ar H; 4,24-Ar H), 7.66 (m, 2,26-Ar H; 3,25-Ar H), 7.55 (d, 10,18-Ar H), 7.40 (d, 11,17-Ar H), 5.41 (t, 28,32-OR-1 CH_2), 5.21 (t, 5,23-OR-1 CH_2), 4.94 (t, 9,19-OR-1 CH_2), 4.69 (t, 12,16-OR-1 CH_2), 2.29 (m, 5,23-OR-2 CH_2; 28,32-OR-2 CH_2), 2.21 (m, 9,19-OR-2 CH_2), 2.12 (m, 12,16-OR-2 CH_2), 1.83 (m, 28,32-OR-3 CH_2), 1.74 (m, 5,23-OR-3 CH_2), 1.57 (m, 9,19-OR-3 CH_2; 12,16-OR-3 CH_2), 1.13 (t, 28,32-OR-3 CH_2), 1.07 (t, 5,23-OR CH_3), 1.01 (t, 9,19-OR CH_3), 0.93 (t, 12,16-OR CH_3), −4.55 (s br, OH). MS-HRFAB exact mass, *m*/*z*: calcd for $C_{72}H_{86}N_8O_{10}Si$ $(M + H)^+$, 1251.6314; found, 1251.6262, 1251.6272.

The compound is a dark-brown solid. It is soluble in toluene, CH_2Cl_2, and pyridine and slightly soluble in hexane.

***t*-$SiN_2P_2(OBu)_8(OH)_2$.** *t*-$SiN_2P_2(OBu)_8(OH)_2$ was prepared by route 1 (43%). UV−vis (λ_{max} (nm), toluene): 763, 859. ^{1}H NMR (C_6D_6): δ 9.24 (m, 9,12,25,28-Ar H), 7.69 (m, 10,11,26,27-Ar H), 7.44 (s, 2,3,-18,19-Ar H), 5.39 (t, 8,13,24,29-OR-1 CH_2), 4.74 (t, 1,4,17,20-OR-1 CH_2), 2.31 (m, 8,13,24,29-OR-2 CH_2), 2.16 (m, 1,4,17,20-OR-2 CH_2), 1.82 (m, 8,13,24,29-OR-3 CH_2), 1.57 (m, 1,4,17,20-OR-3 CH_2), 1.13 (t, 8,13,24,29-OR CH_3), 0.95 (t, 1,4,17,20-OR CH_3).

The compound is a brown solid. It is soluble in toluene, CH_2Cl_2, and pyridine and slightly soluble in hexane.

$SiN_1P_3(OBu)_8(OH)_2$. $SiN_1P_3(OBu)_8(OH)_2$ was prepared by route 1 (69%). UV−vis (λ_{max} (nm), toluene): 762; 793. ^{1}H NMR (C_6D_6): δ 9.21 (m, 23,26-Ar H), 7.67 (m, 24,25-Ar H), 7.53 (d, 2,17-Ar H), 7.52 (s, 9,10-Ar H), 7.40 (d, 3,16-Ar H), 5.34 (t, 22,27-OR-1 CH_2), 4.91 (m, 1,18-OR-1 CH_2; 4,15-OR-1 CH_2), 4.67 (t, 8,11-OR-1 CH_2), 2.29 (m, 22,27-OR-2 CH_2), 2.20 (m, 1,18-OR-2 CH_2; 4,15-OR-2 CH_2; 8,-11-OR-2 CH_2), 1.79 (m, 22,27-OR-3 CH_2), 1.72 (m, 1,18-OR-3 CH_2; 4,15-OR-3 CH_2; 8,11-OR-3 CH_2), 1.17 (t, 22,27-OR CH_3), 1.12 (t, 1,-18-OR CH_3; 4,15-OR CH_3), 0.93 (t, 8,11-OR CH_3).

The compound is a dark-green solid. It is soluble in toluene, CH_2Cl_2, and pyridine and slightly soluble in hexane.

$SiN_0P_4(OBu)_8(OH)_2$ (SiPc$(OBu)_8(OH)_2$). $SiN_0P_4(OBu)_8(OH)_2$ was prepared by route 1 (97%). UV−vis (λ_{max} (nm), toluene): 749. ^{1}H NMR (C_6D_6): δ 7.52 (s, Ar H), 4.87 (t, OR-1 CH_2), 2.17 (m, OR-2 CH_2), 1.69 (m, OR-3 CH_2), 1.05 (t, OR CH_3). ^{13}C NMR (C_6D_6): δ 152.89 (5,7,12,14,19,21,26,28-Ar C), 148.21 (1,4,8,11,15,18,22,25-Ar C), 127.47 (4a,7a,11a,14a,18a,21a,25a,28a-Ar C), 120.76 (2,3,9,10,-16,17,23,24-Ar C), 73.26 (OR-1 C), 32.52 (OR-2 C), 19.94 (OR-3 C), 14.39 (OR-4 C).

The compound is a green solid. It is soluble in toluene, CH_2Cl_2, and pyridine and slightly soluble in hexane.

$SiN_4P_0(OBu)_8(OSi(n\text{-}C_6H_{13})_3)_2$ (SiNc$(OBu)_8(OSi(n\text{-}C_6H_{13})_3)_2$). $SiN_4P_0(OBu)_8(OSi(n\text{-}C_6H_{13})_3)_2$ was prepared by the same type of procedure used for the synthesis of *c*-$SiN_2P_2(OBu)_8(OSi(n\text{-}C_6H_{13})_3)_2$ (**route 2**, see below) (94%). UV−vis (λ_{max} (nm), ϵ (M^{-1} cm^{-1})) (toluene, 1.2 μM): 864, 2.0 × 10^5. ^{1}H NMR (C_6D_6): δ 9.23 (m, 1,4,-10,13,19,22,28,31-Ar H), 7.67 (m, 2,3,11,12,20,21,29,30-Ar H), 5.55 (t, OR-1 CH_2), 2.46 (m, OR-2 CH_2), 1.77 (m, OR-3 CH_2), 1.10 (t, OR CH_3), 0.65 (m, SiR-5 CH_2), 0.39 (m, SiR-3 CH_2; SiR-4 CH_2; SiR CH_3), −0.34 (m, SiR-2 CH_2), −1.33 (m, SiR-1 CH_2). ^{13}C NMR (C_6D_6): δ 151.01 (6,8,15,17,24,26,33,35-Ar C), 148.28 (5,9,14,18,23,27,32,36-Ar C), 131.73 (4a,9a,13a,18a,22a,27a,31a,36a-Ar C), 127.38 (2,3,11,-12,20,21,29,30-Ar C), 124.83 (1,4,10,13,19,22,28,31-Ar C), 122.50 (5a,8a,14a,17a,23a,26a,32a,35a-Ar C), 77.73 (OR-1 C), 34.07 (SiR-4 C), 33.46 (OR-2 C), 31.77 (SiR-3 C), 22.93 (SiR-2 C; SiR-5 C), 20.11 (OR-3 C), 14.84 (SiR-6 C), 14.50 (OR-4 C), 13.99 (SiR-1 C). MS-HRFAB exact mass, *m*/*z*: calcd for $C_{116}H_{166}N_8O_{10}Si_3$ $(M)^+$, 1915.2034; found, 1915.2068, 1915.2067.

The compound is a brown solid. It is very soluble in hexane, toluene, CH_2Cl_2, and pyridine. Its crystals are acicular.

$SiN_3P_1(OBu)_8(OSi(n\text{-}C_6H_{13})_3)_2$. $SiN_3P_1(OBu)_8(OSi(n\text{-}C_6H_{13})_3)_2$ was prepared by route 2 (89%). UV−vis (λ_{max} (nm), ϵ (M^{-1} cm^{-1})) (toluene, 2.2 μM): 820, 1.6 × 10^5; 857, 1.3 × 10^5. ^{1}H NMR (C_6D_6): δ 9.24 (m, 1,4-Ar H; 10,29-Ar H; 13,26-Ar H), 7.67 (m, 2,3-Ar H; 11,28-Ar H; 12,27-Ar H), 7.48 (s, 19,20-Ar H), 5.66 (t, 5,34-OR-1 CH_2), 5.57 (t, 9,30-OR-1 CH_2), 5.15 (t, 14,25-OR-1 CH_2), 4.88 (t, 18,21-OR-1 CH_2), 2.44 (m, 5,34-OR-2 CH_2; 9,30-OR-2 CH_2), 2.33 (m, 14,25-OR-2 CH_2; 18,21-OR-2 CH_2), 1.87 (m, 5,34-OR-3 CH_2; 9,30-OR-3 CH_2), 1.76 (m, 14,25-OR-3 CH_2; 18,21-OR-3 CH_2), 1.18 (t, 5,34-OR CH_3), 1.10 (m, 9,30-OR CH_3; 14,25-OR CH_3), 1.05 (t, 18,21-OR CH_3), 0.75 (m, SiR-5 CH_2), 0.51 (t, SiR CH_3), 0.42 (m, SiR-3 CH_2; SiR-4 CH_2), −0.39 (m, SiR-2 CH_2), −1.41 (m, SiR-1 CH_2). ^{13}C NMR (C_6D_6): δ 152.43 (17,22-Ar C), 151.45 (15,24-Ar C), 151.29 (8,31-Ar C), 150.87 (6,33-Ar C), 150.02 (18,21-Ar C), 149.64 (14,25-Ar C), 147.80 (9,30-Ar C), 146.02 (5,34-Ar C), 132.06 (4a,34a-Ar C), 131.91 (9a,-29a-Ar C), 131.56 (13a,25a-Ar C), 127.53 (2,3-Ar C), 127.40 (11,28-Ar C; 12,27-Ar C), 126.13 (17a,21a-Ar C), 124.89 (1,4-Ar C; 10,29-Ar C), 124.78 (13,26-Ar C), 122.86 (5a,33a-Ar C), 122.51 (8a,30a-Ar C), 122.23 (14a,24a-Ar C), 118.68 (19,20-Ar C), 77.95 (5,34-OR-1 C), 77.85 (9,30-OR-1 C), 77.76 (14,25-OR-1 C), 72.75 (18,21-OR-1 C), 33.97 (SiR-4 C), 33.73 (5,34-OR-2 C), 33.50 (9,30-OR-2 C), 33.45 (14,25-OR-2 C), 32.45 (18,21-OR-2 C), 31.74 (SiR-3 C), 22.98 (SiR-5 C), 22.84 (SiR-2 C), 20.11 (5,34-OR-3 C; 9,30-OR-3 C; 14,25-OR-3 C; 18,21-OR-3 C), 14.66 (SiR-6 C), 14.50 (5,34-OR-4 C; 9,30-OR-4 C; 14,25-OR-4 C; 18,21-OR-4 C), 14.14 (SiR-1 C). MS-HRFAB exact mass, *m*/*z*: calcd for $C_{112}H_{164}N_8O_{10}Si_3$ $(M)^+$, 1865.1878; found, 1865.1915, 1865.1974.

The compound is a brown solid. It is very soluble in toluene, hexane, CH_2Cl_2, and pyridine.

***c*-$SiN_2P_2(OBu)_8(OSi(n\text{-}C_6H_{13})_3)_2$.** A mixture of *c*-$SiN_2P_2(OBu)_8(OH)_2$ (28 mg, 0.020 mmol), $ClSi(n\text{-}C_6H_{13})_3$ (0.50 mL, 1.6 mmol), pyridine (2 mL), and toluene (20 mL) was refluxed for 2 h and evaporated to dryness with a rotary evaporator (∼25 °C, 10 Torr). The solid was chromatographed (wet loading, hexane; Al_2O_3 III, hexane, 1.5 × 20 cm; hexane/toluene; filtration; rotary evaporation (45 °C, ∼20 Torr)), rechromatographed (toluene, ∼0.1 g/mL; BioBeads S-X4 (Bio-Rad Labs, Richmond, CA), 1.5 × 20 cm; toluene; rotary evaporation (45 °C, ∼20 Torr)), dried (60 °C, 25 Torr), and weighed (39 mg, 96%). UV−vis (λ_{max} (nm), ϵ (M^{-1} cm^{-1})) (toluene, 2.0 μM): 804, 1.9 × 10^5. ^{1}H NMR (C_6D_6): δ 9.22 (m, 1,27-Ar H; 4,24-Ar H), 7.66 (m, 2,26-Ar H; 3,25-Ar H), 7.57 (d, 10,18-Ar H), 7.45 (d, 11,17-Ar H), 5.66 (t, 28,32-OR-1 CH_2), 5.52 (t, 5,23-OR-1 CH_2), 5.05 (t, 9,19-OR-1 CH_2), 4.83 (t, 12,16-OR-1 CH_2), 2.41 (m, 5,23-OR-2 CH_2; 28,32-OR-2 CH_2), 2.27 (m, 9,19-OR-2 CH_2; 12,16-OR-2 CH_2), 1.80 (m, 5,23-OR-3 CH_2; 28,32-OR-3 CH_2), 1.69 (m, 9,19-OR-3 CH_2; 12,16-OR-3 CH_2), 1.18 (t, 28,32-OR CH_3), 1.12 (t, 5,23-OR CH_3), 1.10 (t, 9,19-OR CH_3), 1.02 (t, 12,16-OR CH_3), 0.84 (m, SiR-5 CH_2), 0.62 (t, SiR CH_3), 0.46 (m, SiR-3 CH_2; SiR-4 CH_2), −0.47 (m, SiR-2 CH_2), −1.52 (m, SiR-1 CH_2). ^{13}C NMR (C_6D_6): δ 152.70 (13,15-Ar C), 152.43 (8,20-Ar C), 151.75 (12,16-Ar C), 151.28 (9,19-Ar C), 151.19 (6,22-Ar C), 149.42 (29,-31-Ar C), 147.43 (5,23-Ar C), 145.56 (28,32-Ar C), 132.19 (4a,23a-Ar C), 131.88 (27a,32a-Ar C), 127.75 (2,26-Ar C; 3,25-Ar C), 127.09 (12a,15a-Ar C), 126.15 (8a,19a-Ar C), 124.94 (1,27-Ar C), 124.86 (4,-24-Ar C), 122.88 (5a,22a-Ar C), 122.15 (28a,31a-Ar C), 120.70 (10,-18-Ar C), 118.19 (11,17-Ar C), 78.11 (28,32-OR-1 C), 77.85 (5,23-OR-1 C), 73.50 (9,19-OR-1 C), 72.58 (12,16-OR-1 C), 33.84 (28,32-OR-2 C; SiR-4 C), 33.49 (5,23-OR-2 C), 32.57 (9,19-OR-2 C), 32.43 (12,16-OR-2 C), 31.69 (SiR-3 C), 23.01 (SiR-5 C), 22.72 (SiR-2 C), 20.13 (5,23-OR-3 C; 28,32-OR-3 C), 20.04 (9,19-OR-3 C; 12,16-OR-3 C), 14.46 (5,23-OR-4 C; 9,19-OR-4 C; 12,16-OR-4 C; 28,32-OR-4 C; SiR-6 C), 14.26 (SiR-1 C). MS-HRFAB exact mass, *m*/*z*: calcd for $C_{108}H_{162}N_8O_{10}Si_3$ $(M + H)^+$, 1816.1800; found, 1816.1767, 1816.1758.

The compound is a dark-green solid. It is very soluble in hexane, toluene, CH_2Cl_2, and pyridine.

***t*-$SiN_2P_2(OBu)_8(OSi(n\text{-}C_6H_{13})_3)_2$.** *t*-$SiN_2P_2(OBu)_8(OSi(n\text{-}C_6H_{13})_3)_2$ was prepared by route 2 (79%). UV−vis (λ_{max} (nm), ϵ (M^{-1} cm^{-1})) (toluene, 1.5 μM): 760, 1.5×10^5; 851, 1.2×10^5. ^1H NMR (C_6D_6): δ 9.24 (m, 9,12,25,28-Ar H), 7.68 (m, 10,11,26,27-Ar H), 7.50 (s, 2,3,-18,19-Ar H), 5.62 (t, 8,13,24,29-OR-1 CH_2), 4.89 (t, 1,4,17,20-OR-1 CH_2), 2.38 (m, 8,13,24,29-OR-2 CH_2), 2.32 (m, 1,4,17,20-OR-2 CH_2), 1.84 (m, 8,13,24,29-OR-3 CH_2), 1.70 (m, 1,4,17,20-OR-3 CH_2), 1.18 (t, 8,13,24,29-OR CH_3), 1.04 (t, 1,4,17,20-OR CH_3), 0.85 (m, SiR-5 CH_2), 0.62 (t, SiR CH_3), 0.45 (m, SiR-3 CH_2; SiR-4 CH_2), −0.49 (m, SiR-2 CH_2), −1.56 (m, SiR-1 CH_2). ^{13}C NMR (C_6D_6): δ 152.67 (5,-16,21,32-Ar C), 151.12 (1,4,17,20-Ar C), 149.02 (7,14,23,30-Ar C; 8,-13,24,29-Ar C), 131.37 (8a,12a,24a,28a-Ar C), 127.75 (10,11,26,27-Ar C), 126.95 (4a,16a,20a,32a-Ar C), 126.41 (7a,13a,23a,29a-Ar C), 124.82 (9,12,25,28-Ar C), 119.52 (2,3,18,19-Ar C), 78.00 (8,13,24,-29-OR-1 C), 72.86 (1,4,17,20-OR-1 C), 33.81 (SiR-4 C), 33.73 (8,-13,24,29-OR-2 C), 32.47 (1,4,17,20-OR-2 C), 31.68 (SiR-3 C), 23.00 (SiR-5 C), 22.69 (SiR-2 C), 20.10 (1,4,17,20-OR-3 C; 8,13,24,29-OR-3 C), 14.49 (1,4,17,20-OR-4 C; 8,13,24,29-OR-4 C), 14.41 (SiR-6 C), 14.26 (SiR-1 C). MS-HRFAB exact mass, *m*/*z*: calcd for $C_{108}H_{162}N_8O_{10}Si_3$ $(M + H)^+$, 1816.1800; found, 1816.1742, 1816.1775.

The compound is a brown solid. It is very soluble in hexane, toluene, CH_2Cl_2, and pyridine.

$SiN_1P_3(OSi(n\text{-}C_6H_{13})_3)_2$. $SiN_1P_3(OSi(n\text{-}C_6H_{13})_3)_2$ was prepared by route 2 (69%). UV−vis (λ_{max} (nm), ϵ (M^{-1} cm^{-1})) (toluene, 2.1 μM): 761, 2.2×10^5; 794, 1.5×10^5. ^1H NMR (C_6D_6): δ 9.22 (m, 23,26-Ar H), 7.67 (m, 24,25-Ar H), 7.58 (d, 2,17-Ar H), 7.55 (s, 9,10-Ar H), 7.45 (d, 3,16-Ar H), 5.62 (t, 22,27-OR-1 CH_2), 5.06 (t, 1,18-OR-1 CH_2), 5.01 (t, 4,15-OR-1 CH_2), 4.83 (t, 8,11-OR-1 CH_2), 2.36 (m, 22,27-OR-2 CH_2), 2.28 (m, 1,18-OR-2 CH_2; 4,15-OR-2 CH_2; 8,11-OR-2 CH_2), 1.78 (m, 22,27-OR-3 CH_2), 1.68 (m, 1,18-OR-3 CH_2; 4,15-OR-3 CH_2; 8,11-OR-3 CH_2), 1.17 (t, 22,27-OR CH_3), 1.12 (m, 1,18-OR CH_3; 4,-15-OR CH_3), 1.02 (t, 8,11-OR CH_3), 0.92 (m, SiR-5 CH_2), 0.72 (t, SiR CH_3), 0.55 (m, SiR-4 CH_2), 0.42 (m, SiR-3 CH_2), −0.58 (m, SiR-2 CH_2), −1.67 (m, SiR-1 CH_2). ^{13}C NMR (C_6D_6): δ 152.95 (7,12-Ar C), 152.74 (5,14-Ar C; 19,30-Ar C), 152.69 (21,28-Ar C), 151.63 (1,-18-Ar C; 4,15-Ar C; 8,11-Ar C), 150.20 (22,27-Ar C), 131.99 (22a,-26a-Ar C), 127.35 (24,25-Ar C), 127.11 (7a,11a-Ar C), 126.94 (21a,27a-Ar C), 126.43 (4a,14a-Ar C; 18a,30a-Ar C), 124.89 (23,26-Ar C), 121.57 (2,17-Ar C), 120.17 (3,16-Ar C), 118.96 (9,10-Ar C), 78.15 (22,27-OR-1 C), 73.67 (1,18-OR-1 C; 4,15-OR-1 C), 72.65 (8,11-OR-1 C), 33.70 (22,27-OR-2 C; SiR-4 C), 32.61 (1,18-OR-2 C), 32.54 (4,-15-OR-2 C), 32.44 (8,11-OR-2 C), 31.64 (SiR-3 C), 23.04 (SiR-5 C), 22.56 (SiR-2 C), 20.12 (1,18-OR-3 C; 22,27-OR-3 C), 20.03 (4,15-OR-3 C; 8,11-OR-3 C), 14.39 (1,18-OR-4 C; 4,15-OR-4 C; 8,11-OR-4 C; 22,27-OR-4 C; SiR-6 C), 14.20 (SiR-1 C). MS-HRFAB exact mass, *m*/*z*: calcd for $C_{104}H_{160}N_8O_{10}Si_3$ $(M)^+$, 1765.1565; found, 1765.1583, 1765.1527.

The compound is a dark-green solid. It is very soluble in hexane, toluene, CH_2Cl_2, and pyridine.

$SiN_0P_4(OBu)_8(OSi(n\text{-}C_6H_{13})_3)_2$ ($SiPc(OBu)_8(OSi(n\text{-}C_6H_{13})_3)_2$). $SiN_0P_4(OBu)_8(OSi(n\text{-}C_6H_{13})_3)_2$ was prepared by route 2 (88%). UV−vis (λ_{max} (nm), ϵ (M^{-1} cm^{-1})) (toluene, 1.7 μM): 747, 2.3×10^5. ^1H NMR (C_6D_6): δ 7.57 (s, Ar H), 5.03 (t, OR-1 CH_2), 2.27 (m, OR-2 CH_2), 1.77 (m, OR-3 CH_2), 1.11 (t, OR CH_3), 0.99 (m, SiR-5 CH_2), 0.82 (t, SiR CH_3), 0.59 (m, SiR-4 CH_2), 0.39 (m, SiR-3 CH_2), −0.70 (m, SiR-2 CH_2), −1.83 (m, SiR-1 CH_2). ^{13}C NMR (C_6D_6): δ 153.02 (5,7,12,14,19,21,26,28-Ar C), 148.16 (1,4,8,11,15,18,22,25-Ar C), 127.38 (4a,7a,11a,14a,18a,21a,25a,28a-Ar C), 121.07 (2,3,9,10,16,17,-23,24-Ar C), 73.53 (OR-1 C), 33.58 (SiR- 4C), 32.58 (OR-2 C), 31.58 (SiR-3 C), 23.07 (SiR-5 C), 22.40 (SiR-2 C), 20.02 (OR-3 C), 14.50 (SiR-6 C), 14.43 (OR-4 C), 13.91 (SiR-1 C). MS-HRFAB exact mass, *m*/*z*: calcd for $C_{100}H_{158}N_8O_{10}Si_3$ $(M)^+$, 1715.1408; found, 1715.1384, 1715.1453.

The compound is a green solid. It is very soluble in hexane, toluene, CH_2Cl_2, and pyridine.

(B) Characterization Spectra. The NMR spectra were taken with a Varian Gemini 300 spectrometer (Varian Associates, Inc.). The ground state characterization visible−near-infrared spectra were taken with a Varian Cary 1 UV−vis spectrophotometer interfaced to a Gateway 2000 386-25 computer (Gateway 2000, North Sioux City, SD). The mass spectra were determined by the Midwest Center for Mass Spectrometry (University of Nebraska−Lincoln, Lincoln, NE) and the Washington University Resource for Biological and Bio-Organic Mass Spectrometry (St. Louis, MO).

(C) Other Materials. Benzene (HPLC reagent, Baker Chemical Co.) and benzophenone (certified reagent, Fisher Scientific Co.) were used as received. 2-Hydroxyethyl-7,12,17-tris(methoxyethyl)porphycene (HEP_n) of >97% purity was kindly provided by Professor E. Vogel (Institute of Organic Chemistry, University of Cologne).

(D) Photophysical Measurements. Flash photolysis experiments were performed with the third harmonic (355 nm) of a Continuum Surelite I Q-switched Nd:YAG laser which provided 10 ns pulses. In some instances excitation was carried out at 605 nm using an optical parameter oscillator (Opotek *MagicPrism*) system pumped by the third harmonic of the Nd:YAG laser. Transient absorbances were monitored at right angles to the laser beam using a computer-controlled kinetic spectrophotometer which has been described.[9]

Phosphorescence spectra of the photosensitizers were measured using a Bruker IFS66 interferometer-based instrument with a Bruker RFA 106 Raman accessory, adapted for luminescence measurements and described elsewhere.[30]

Triplet−triplet molar extinction coefficients (ϵ_{TT}) were measured by the ground state complete conversion method.[31] The values of ΔA at the saturation level were determined at several sensitizer concentrations and plotted in the Beer−Lambert manner. The slope of such plots corresponds to the value of the difference between the extinction coefficients of the ground and excited states of the test compound. Correcting this with the known value of the ground state compound leads to the absolute value of ϵ_{TT}.

Triplet quantum yields (Φ_T) were determined by a comparative method[32] using benzophenone in benzene as reference ($\Phi^r_T = 1.0$; ϵ^r_{TT} = 7200 M^{-1} cm^{-1} at 530 nm). Because triplet quantum yield determinations by laser flash photolysis have been reported to be sensitive to the incident laser intensity,[32] the measurements were made at a series of laser intensities and the following expression was employed:

$$\Phi^x_T = \Phi^r_T (k_x/k_r) (\epsilon^r_T/\epsilon^x_T) \quad (1)$$

where k_x and k_r represent the slopes of the linear variation of the optical density at the $T_1 \rightarrow T_n$ spectral maximum with laser intensity for the unknown and reference solutions respectively, and ϵ^x_T and ϵ^r_T are the molar extinction coefficients of this transition at the wavelength of observation.

Time-resolved singlet oxygen luminescence (1.27 μm) signals were measured using a germanium photodiode-amplifier-based system cooled to 77 K (Applied Detector Corporation, model 403L). A complete description of the instrumentation is given elsewhere.[33] Typically, 100 laser shots were averaged together at each of a series of different laser intensities selected by a rotating polarizer attenuator calibrated with a power meter. The time profiles observed from such experiments are usually a composite of a fast component resulting from residual scattered laser light and near-IR fluorescence processed through the time constant of the detector system (*ca*. 600 ns) and a slower component that arises from the singlet oxygen luminescence decay. Fitting the slow component with an exponential and extrapolating back to time 0 provides a measure of the $O_2(^1\Delta_g)$ concentration prior to the onset of the decay (L_0). Measurements of L_0 were made at a series of laser intensities for both the test solutions and for a solution of benzophenone in benzene ($\Phi_\Delta = 0.29$)[34] having the same absorbance at 355 nm. These provided values of $L_0(x)$ and $L_0(r)$ for the series of laser intensities, where x and r refer to the test solution and the reference solution (benzophenone), respectively. At low laser intensities, the plots of $L_0(x)$ *vs* $L_0(r)$ were linear. From these plots, the slopes k_{x-r} were extracted and used to calculate the quantum yield of singlet oxygen of the unknown solution under the prevailing conditions, according to the expression

(30) Wessels, J. M.; Charlesworth, P.; Rodgers, M. A. J. *Photochem. Photobiol*. **1995**, *61*, 350.

(31) Bensasson, R.; Land, E. J.; Truscott, T. G. *Flash Photolysis and Pulsed Radiolysis: Contributions to the Chemistry of Biology and Medicine*; Pergamon Press: Oxford, 1983.

(32) Bensasson, R.; Goldschmitt, C. R.; Land, E. J.; Truscott, T. G. *Photochem. Photobiol*. **1977**, *28*, 277.

(33) Zhang, X.; Rodgers, M. A. J. *J. Phys. Chem*. **1995**, *99*, 12797.

(34) Gorman, A. A.; Hamblett, I.; Rodgers, M. A. J. *J. Am. Chem. Soc*. **1984**, *106*, 4679.

Table 1. Q-Band Maxima Associated with $H_2N_{4-x}P_x(OBu)_8$, $SiN_{4-x}P_x(OBu)_8(OH)_2$, and $SiN_{4-x}P_x(OBu)_8(OSi(n\text{-}C_6H_{13})_3)_2$

	range		band				compound		
	limits (nm)	span (nm)	position (nm)	ϵ (M^{-1} $cm^{-1}/10^5$)	type[a]	Δ[b]	ring	core	ligands
1	739−763	24	739	0.95	d		N_0P_4	H	
			747	2.3	s	8	N_0P_4	Si	$OSiR_3$
			749		s	2	N_0P_4	Si	OH
			750	0.98	d	1	*t*-N_2P_2	H	
			756	0.82	d	6	N_1P_3	H	
			760	1.5	d	4	*t*-N_2P_2	Si	$OSiR_3$
			761	2.2	d	1	N_1P_3	Si	$OSiR_3$
				1.1	d	1	N_0P_4	H	
			762		d	1	N_1P_3	Si	OH
			763		d	1	*t*-N_2P_2	Si	OH
2	793-825	32	793		d	30	N_1P_3	Si	OH
			794	1.5	d	1	N_1P_3	Si	$OSiR_3$
			802	0.66	d	8	N_1P_3	H	
			804	1.9	s	2	*c*-N_2P_2	Si	$OSiR_3$
			805		s	1	*c*-N_2P_2	Si	OH
			807	1.9	s	2	*c*-N_2P_2	H	
			814	0.99	d	7	N_3P_1	H	
			820	1.6	d	6	N_3P_1	Si	$OSiR_3$
			825		d	5	N_3P_1	Si	OH
3	851-865	14	851	1.2	d	26	*t*-N_2P_2	Si	$OSiR_3$
				0.89	d	0	N_3P_1	H	
			852	0.75	d	1	*t*-N_2P_2	H	
			857	1.3	d	5	N_3P_1	Si	$OSiR_3$
			859		d	2	*t*-N_2P_2	Si	OH
			861		d	2	N_3P_1	Si	OH
			862	2.0	s	1	N_4P_0	H	
			864	2.0	s	2	N_4P_0	Si	$OSiR_3$
			865		s	1	N_4P_0	Si	OH

[a] From single (s) maximum band; from double (d) maximum band. [b] From preceding maximum (nm).

$$k_{x-r} = (\Phi^x{}_\Delta \eta^x A^x)/(\Phi^r{}_\Delta \eta^r A^r) \quad (2)$$

where A is the absorbance at the excitation wavelength, $\Phi^x{}_\Delta$ is the singlet oxygen quantum yield ($\Phi^r{}_\Delta = 0.29$) and η the quenching efficiency given by

$$\eta = k_{T\Sigma}[O_2]/(k_o + k_{T\Sigma}[O_2]) \quad (3)$$

where k_o is the decay rate constant of the triplet in argon-saturated solutions and $k_{T\Sigma}$ is the bimolecular rate constant for quenching of the triplet state by oxygen.

Results and Discussion

Syntheses. In the past, silicon phthalocyanines generally have been made by the cyclization of a ring precursor, often a diiminoisoindoline, around a silicon core precursor, generally a chlorosilane. An example of this route is the following:[35]

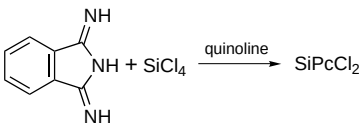

In this work, silicon phthalocyanines were made instead by insertion of a part of a silicon core precursor, $HSiCl_3$, into a metal-free phthalocyanine, for example:

$$H_2N_3P_1(OBu)_8 + HSiCl_3 \xrightarrow[C_6H_5CH_3]{N(C_4H_9)_3,} \xrightarrow{H_2O} SiN_3P_1(OBu)_8(OH)_2$$

Since this route entails the use of a reaction mixture containing tri-*n*-butylamine, it is likely that it involves the reaction of the ion pairs $[HN(C_4H_9)_3]^+[HN_{4-x}P_x(OBu)_8]^-$ or $[HN(C_4H_9)_3]_2{}^+[N_{4-x}P_x(OBu)_8]^{2-}$ with the $HSiCl_3$ or a species derived from it.

This route is similar to a route recently reported for the synthesis of silicon porphyrins.[36,37] In this latter route, the compounds are made by insertion of a part of $HSiCl_3$ into a dilithioporphyrin, for example $[Li_2(THF)_2]^{2+}[TPP]^{2-}$. Thus,

$$[Li_2(THF)_2]^{2+}[TPP]^{2-} + HSiCl_3 \xrightarrow{CH_2Cl_2} SiTPPCl_2$$

The new route to silicon phthalocyanines is an attractive alternative to the route generally used because it is simple and works well.

Visible−Near-Infrared Spectra. The ground state Q-band maxima and extinction coefficients of the series of compounds made are collected in Table 1. As anticipated, all the compounds absorb strongly in the deep-red region of the electromagnetic spectrum, with the Q-band maxima spanning the range from 739 to 865 nm. The visible−near-infrared spectra in benzene of the *cis* and *trans* isomers of $SiN_2P_2(OBu)_8(OSi(n\text{-}C_6H_{13})_3)_2$, the compounds upon which photophysical studies were performed (*vide infra*), are shown in Figure 2. Beer−Lambert law plots for this isomeric pair showed excellent linearity in the range of concentration investigated (up to 150 μM), indicating no evidence for aggregation in the ground state.

The Q-band position or average Q-band position in the three series shifts to the red as the number of benzo rings increases, as expected in view of the increasing size of the delocalized system.

The presence of single maxima in the Q-bands of phthalocyanine-type compounds of D_{4h} symmetry and often the presence of double maxima in the Q-bands of such compounds of lower symmetry is well-known. In the bands of the D_{4h} compounds, the presence of single maxima is attributed to an electronic transition between a filled π molecular orbital and a

(35) Lowery, M. K.; Starshak, A. J.; Esposito, J. N.; Krueger, P. C.; Kenney, M. E. *Inorg. Chem.* **1965**, *4*, 128.

(36) Kane, K. M.; Lemke, F. R.; Petersen, J. L. *Inorg. Chem.* **1995**, *34*, 4085.

(37) Kane, K. M.; Lemke, F. R. *Abstracts of Papers*; 210th National Meeting of the American Chemical Society, Chicago, IL; American Chemical Society: Washington, DC, 1995; INORG 667.

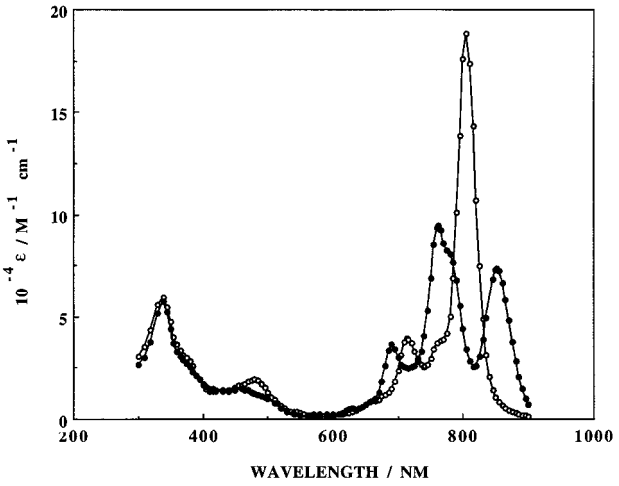

Figure 2. Ground state absorption spectra of *cis* isomer (○) and *trans* isomer (●) in benzene.

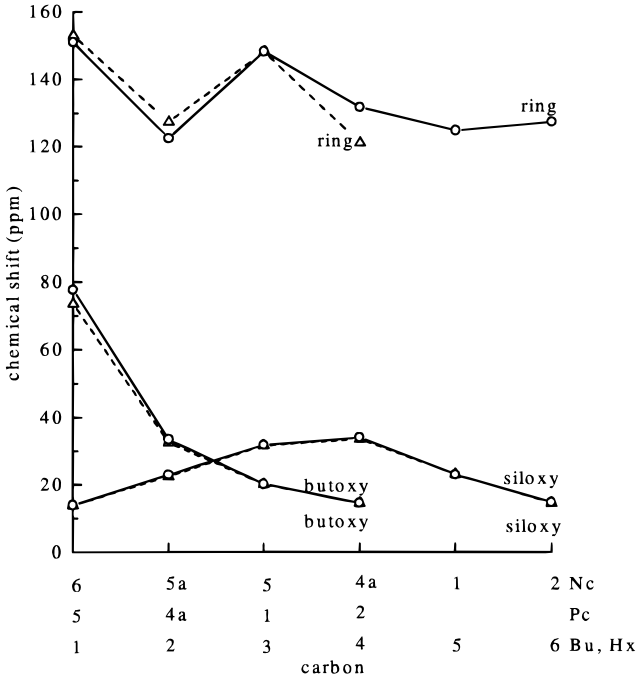

Figure 3. Positions of ring, butoxy, and hexylsiloxy carbons of $SiN_4P_0(OSi(n\text{-}C_6H_{13})_3)_2$ (○) and $SiN_0P_4(OSi(n\text{-}C_6H_{13})_3)_2$ (△).

pair of empty, higher energy, doubly degenerate π molecular orbitals. In the bands of the lower symmetry compounds, the presence of two maxima, where such is the case, is commonly attributed to transitions between a π molecular orbital, which is like the filled molecular orbital in the D_{4h} compounds, and a pair of empty molecular orbitals, which are like the pair of empty molecular orbitals of the D_{4h} compounds except that, because of the lower symmetry of the compounds, they are non-degenerate.[38−42]

Since the compounds $SiN_4P_0(OBu)_8(OH)_2$, $SiN_4P_0(OBu)_8(OSi(n\text{-}C_6H_{13})_3)_2$, $SiN_0P_4(OBu)_8(OH)_2$, and $SiN_0P_4(OBu)_8(OSi(n\text{-}C_6H_{13})_3)_2$ are of approximately D_{4h} symmetry, the presence of single maxima in their Q-bands can be understood. Likewise, since the compounds in the three series $H_2N_3P_1(OBu)_8-H_2N_1P_3(OBu)_8$, $SiN_3P_1(OBu)_8(OH)_2-SiN_1P_3(OBu)_8(OH)_2$, and $SiN_3P_1(OBu)_8(OSi(n\text{-}C_6H_{13})_3)_2-SiN_1P_3(OBu)_8(OSi(n\text{-}C_6H_{13})_3)_2$ are of less than D_{4h} symmetry and since $H_2N_4P_0(OBu)_8$ and $H_2N_0P_4(OBu)_8$ probably also are of less than D_{4h} symmetry on a spectroscopic time scale, the presence of double maxima in their Q-bands, where observed, can be understood. The presence of apparent single maxima in the spectra of $H_2N_4P_0(OBu)_8$, *c*-$H_2N_2P_2(OBu)_8$, *c*-$SiN_2P_2(OBu)_8(OH)_2$, and *c*-$SiN_2P_2(OBu)_8(OSi(n\text{-}C_6H_{13})_3)_2$ probably is due to accidental band overlaps.

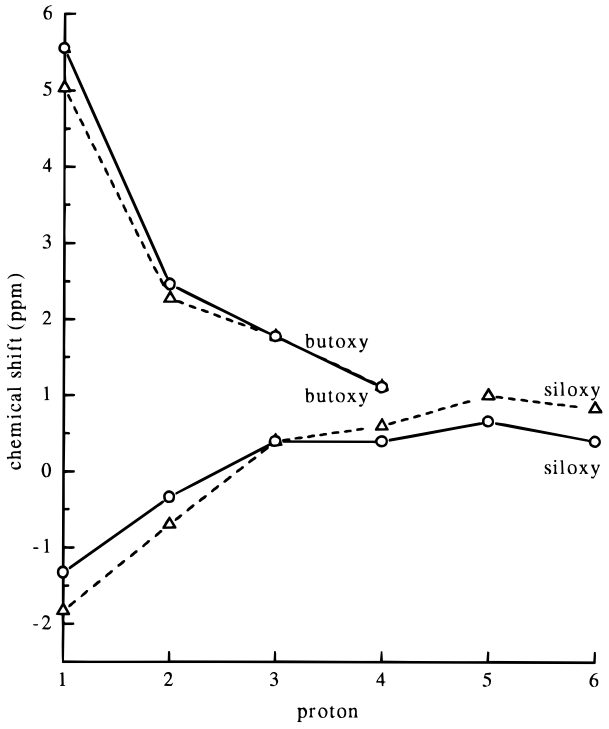

Figure 4. Positions of butoxy and hexylsiloxy protons of $SiN_4P_0(OSi(n\text{-}C_6H_{13})_3)_2$ (○) and $SiN_0P_4(OSi(n\text{-}C_6H_{13})_3)_2$ (△).

The 28 maxima of the Q-bands of the 18 compounds made can be grouped into three sets. The first contains 10 maxima in a 24 nm range running from 739 to 763 nm. The second contains 9 maxima in a 32 nm range running from 793 to 825 nm, and the third contains 9 maxima in a 14 nm range running from 851 to 865 nm, Table 1. The bands of the second set are of particular interest because they have maxima that are near or in the range which is most common for the line of the ordinary GaAlAs diode laser, 800−810 nm. Of the bands within this set, the 804, 805, and 807 nm bands are of the most interest because they are sharp, are very intense, and have maxima in the part of the diode laser range which is most common.

Since the 804, 805, and 807 nm bands belong to *c*-$SiN_2P_2(OBu)_8(OSi(n\text{-}C_6H_{13})_3)_2$, *c*-$SiN_2P_2(OBu)_8(OH)_2$, and *c*-$H_2N_2P_2(OBu)_8$, respectively, these compounds become of particular interest. The potential of these compounds is enhanced by their very high solubility in common organic solvents (*e.g.*, toluene) and their general stability. It should be possible, if desired, to obtain compounds with bands shifted by a few nanometers from those in the three sets by small alterations of the axial ligands or peripheral groups of the appropriate compounds.

NMR Spectra. Designation of Atom Positions. For discussion of the NMR spectra, it is useful to classify the ring atoms by the type of arm in which they are located and the lowest number of the corresponding atom in metal-free naphthalocyanine or phthalocyanine, to classify the butoxy atoms by the type of arm to which they are attached and their numerical position in the chain, and to classify the hexylsiloxy atoms by

(38) Solovev, K. N.; Mashenkov, V. A.; Kachura, T. F. *Opt. Spectrosc.* (*Engl. Transl.*) **1969**, *27*, 24.
(39) Konami, H.; Ikeda, Y.; Hatano, M.; Mochizuki, K. *Mol. Phys.* **1993**, *80*, 153.
(40) Margaron, P.; Gaspard, S.; van Lier, J. E. *J. Chromatogr.* **1993**, *634*, 57.
(41) Kudrevich, S. V.; Ali, H.; van Lier, J. E. *J. Chem. Soc., Perkin Trans. 1* **1994**, 2767.
(42) Linssen, T. G.; Hanack, M. *Chem. Ber.* **1994**, *127*, 2051.

Table 2. Variations in Resonance Positions of Matching and Comparable Atoms in All Compound Pairs, Sets, and Series (ppm)

	carbon			proton		
	pairs	series	both	sets	series	both
Nc 2	0.39	0.40	0.40	0.05	0.05	0.05
1	0.80	0.78	0.80	0.03	0.05	0.05
4a	0.98	0.82	0.98			
5	4.77	4.64	4.77			
5a	1.44	4.79	4.79			
6	1.70	3.67	3.67			
Pc 2	1.40	3.38	3.38	0.06	0.16	0.16
1	1.48	3.59	3.59			
4a	2.73	4.54	4.54			
5	1.23	1.43	1.43			
Nc BuO 1	0.65	0.42	0.65	0.31	0.51	0.51
2	0.23	0.39	0.39	0.13	0.14	0.14
3	0.22	0.26	0.26	0.10	0.21	0.21
4	0.04	0.11	0.11	0.08	0.16	0.16
Pc BuO 1	0.67	1.09	1.09	0.16	0.27	0.27
2	0.12	0.22	0.22	0.16	0.16	0.16
3	0.08	0.12	0.12	0.13	0.20	0.20
4	0.06	0.11	0.11	0.10	0.19	0.19
HxSi 1		0.35	0.35		0.50	0.50
2		0.53	0.53		0.36	0.36
3		0.19	0.19		0.07	0.07
4		0.49	0.49		0.20	0.20
5		0.14	0.14		0.34	0.34
6		0.45	0.45		0.43	0.43

their numerical position in the chain. Thus, for example, the 21a,27a carbons of $H_2N_1P_3(OBu)_8$ become classified as Nc 5a carbons, and the α carbons of the butoxy chains on the naphthalocyanine arm of this compound as Nc BuO 1 carbons.

^{13}C NMR Spectra. The maximum variation in the resonance position of matching and comparable naphthalocyanine and phthalocyanine arm butoxy carbons and hexylsiloxy carbons in six matching compound pairs[43] and two matching compound series[44] is small (1.1 ppm, Table 2). In contrast, the maximum variation in the resonance position of the matching and comparable naphthalocyanine and phthalocyanine arm ring carbons in the six pairs and two series is substantial (4.8 ppm). Further, the largest variations of both the matching and comparable ring carbons in the pairs and series are associated with the inner carbons. These results are consistent with the known greater variability of the electron density in aromatic systems. In addition, they indicate that the variability of the electron density in the macrocycles is greater near their centers, as expected.

The carbons of compounds that are adjacent to N or O are at lower field than those that are one atom away, and the carbons that are adjacent to Si or methyl C are at higher field than those that are one atom away (Figure 3). This fits with the known electron-shifting abilities of N, O, Si, and methyl C.

The existence of unsplit resonances for the hexyl carbons of the siloxysilicon compounds shows that the siloxy groups in these compounds rotate freely on an NMR time scale when the compounds are in solution. This is consistent with the free rotation of the siloxy groups in compounds such as SiPc(OSi(n-$C_6H_{13})_3)_2$ on an NMR time scale when the compounds are in solution.[45]

^{1}H NMR Spectra. The variations in the positions of the matching and comparable naphthalocyanine and phthalocyanine arm butoxy protons, hexylsiloxy protons, and naphthalocyanine and phthalocyanine arm ring protons in six matching compound sets[46] and three matching compound series[47] are all relatively small (<0.6 ppm, Table 2). These results indicate, as expected, that the shapes of the ring-current fields in the planes around the naphthalocyanine arms are similar from arm to arm and that the fields in the planes around the phthalocyanine arms likewise are similar from arm to arm. They further indicate that the fields above the macrocycles are similar and, thus, that the fields above the $N_3P_1(OBu)_8-N_1P_3(OBu)_8$ rings have the expected shape.[48,49]

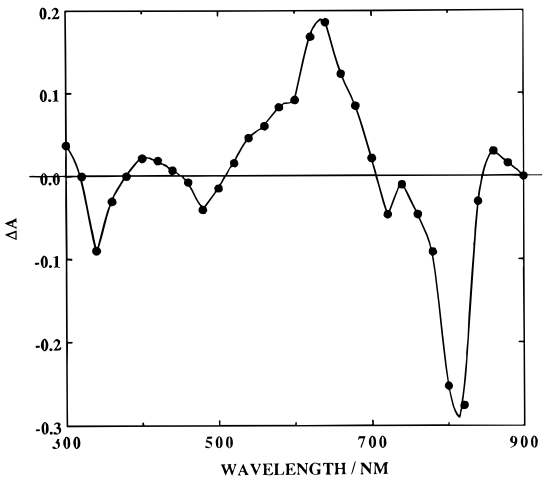

Figure 5. Transient absorption spectrum of *cis* isomer (2 μM) in argon-saturated benzene solution at 2.5 μs postlaser excitation.

The positions of the butoxy and hexylsiloxy protons (Figure 4) provide evidence that the full ring-current fields of the $N_3P_1(OBu)_8-N_1P_3(OBu)_8$ rings have the expected shape if allowance is made for the electronegativities of Si and O.

The presence of single multiplets for the hexyl protons of the siloxysilicon compounds provides further evidence that the siloxy groups in these compounds rotate freely when the compounds are in solution. The fact that NH protons of the series $H_2N_3P_1(OBu)_8$, c-$H_2N_2P_2(OBu)_8$, and $H_2N_1P_3(OBu)_8$ give only one resonance shows that these NH protons circulate freely in the core of the compounds on an NMR time scale when the compounds are in solution.

Photophysical Studies. As indicated above, it is c-$SiN_2P_2(OBu)_8(OSi(n\text{-}C_6H_{13})_3)_2$ that has a single, intense Q-band peak at 804 nm, making it a very interesting species as photodynamic photosensitizer and as a photorecording agent. Because of this, it was decided to examine the photophysical properties of this isomer alongside those of the *trans* isomer, which, as already noted, possesses a pair of Q-band peaks at 760 and 850 nm. The energy of the lowest singlet excited state of the *trans* isomer is therefore expected to be significantly lower than that of the *cis* isomer. The peak-to-peak difference of 46 nm corresponds to an energy difference of *ca*. 1.9 kcal mol^{-1}.

Transient Absorption Studies. Figure 5 shows the absorption spectrum measured at 2.5 μs after a 10 ns pulse of 355 nm radiation incident upon an argon-saturated solution of the *cis* isomer (2 μM) in benzene. The negative absorptions at 340, 490, and 804 nm correspond to bleaching of the ground state absorption peaks (see Figure 2). The positive absorption near 640 nm is reminiscent of similar maxima in the $T_1 \rightarrow T_n$ spectra of other members of the Pc and Nc families.[3-7] At low laser intensity, the 640 nm absorption decayed exponentially with a

(43) $H_2N_{4-x}P_x(OBu)_8$ and $SiN_{4-x}P_x(OBu)_8(OSi(n\text{-}C_6H_{13})_3)_2$ (for example, $H_2N_1P_3(OBu)_8$ and $SiN_1P_3(OBu)_8(OSi(n\text{-}C_6H_{13})_3)_2$).

(44) $H_2N_4P_0(OBu)_8$ to $H_2N_0P_4(OBu)_8$ and $SiN_4P_0(OBu)_8(OSi(n\text{-}C_6H_{13})_3)_2$ to $SiN_0P_4(OBu)_8(OSi(n\text{-}C_6H_{13})_3)_2$).

(45) Wheeler, B. L.; Nagasubramanian, G.; Bard, A. J.; Schechtman, L. A.; Dininny, D. R.; Kenney, M. E. *J. Am. Chem. Soc.* **1984**, *106*, 7404.

(46) $H_2N_{4-x}P_x(OBu)_8$, $SiN_{4-x}P_x(OBu)_8(OH)_2$, and $SiN_{4-x}P_x(OBu)_8(OSi(n\text{-}C_6H_{13})_3)_2$.

(47) $H_2N_4P_0(OBu)_8$ to $H_2N_0P_4(OBu)_8$, $SiN_4P_0(OBu)_8(OH)_2$ to $SiN_0P_4(OBu)_8(OH)_2$, and $SiN_4P_0(OBu)_8(OSi(n\text{-}C_6H_{13})_3)_2$ to $SiN_0P_4(OBu)_8(OSi(n\text{-}C_6H_{13})_3)_2$.

(48) Janson, T. R.; Kane, A. R.; Sullivan J. F.; Knox, K.; Kenney, M. E. *J. Am. Chem. Soc.* **1969**, *91*, 5210.

(49) Maskasky, J. E.; Mooney, J. R.; Kenney, M. E. *J. Am. Chem. Soc.* **1972**, *94*, 2132.

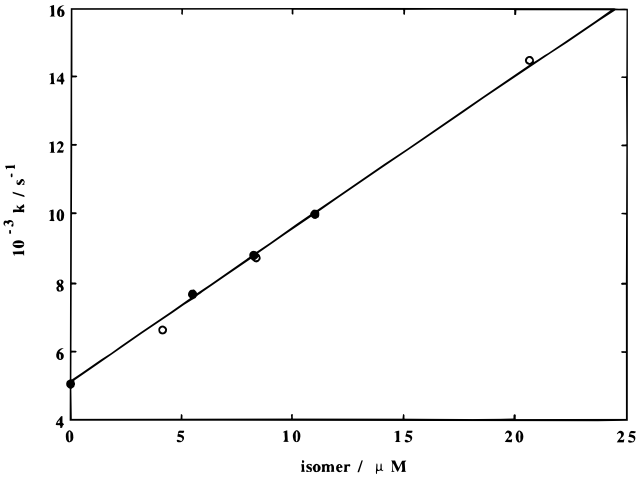

Figure 6. Variation of the rate constant for quenching of the T_1 state of HPE_n in benzene by the *cis* (●) and *trans* (○) isomers. [HPE] = 36 μM.

Table 3. Photophysical Data

compound	τ_T (s)	λ^T_{max} (nm)	ϵ_{T-T} (M^{-1} cm^{-1})	Φ_T	Φ_Δ	$k_{T\Sigma}$ (M^{-1} s^{-1})
cis	105	640	30 000	0.20	0.20	1.19×10^8
trans	72	660	36 780	0.21	0.18	1.6×10^7

lifetime of 105 μs. Similar experiments with the *trans* isomer showed similar spectral features with a prominent $\lambda_{max} = 660$ nm and a triplet lifetime of 72 μs, significantly smaller than that of the *cis* isomer. Both *cis*- and *trans*-derived transients were quenched by ground state molecular oxygen. More detail of this oxygen quenching appears below.

When a benzene solution contained a porphycene such as HPE_n (36 μM) in addition to the *cis* or *trans* isomers and excitation was carried out at 605 nm, where the HPE_n absorption is dominant, the porphycene triplet state ($\lambda_T = 390$ nm) was observed to decay more rapidly than in the absence of the *cis* and *trans* isomers. At the same time, a concomitant formation of the 640 nm absorption was observed for the *cis* isomer. This phenomenon is consistent with the transfer of energy from the higher-lying porphycene triplet to the lower-lying *cis* isomer triplet. This evidence, plus the similarity of the transient absorbances to those of other compounds in the naphthalocyanine and phthalocyanine families and the quenching by oxygen, allows the assignment of the species absorbing at 640 and 660 nm to the T_1 states of the *cis* and *trans* isomers, respectively. The bimolecular rate constant for the triplet energy transfer in benzene was determined to be identical for both isomers (Figure 6) and to be equal to 4.46×10^8 M^{-1} s^{-1}. This value is an order of magnitude lower than that typical of exothermic triplet energy transfer and may signify that the *cis* and *trans* isomers encounter some steric difficulty in attaining optimum approach distance and geometry for energy transfer.[5]

Experiments were conducted as outlined in the Experimental Section to determine the absolute extinction coefficients for the $T_1 \rightarrow T_n$ transition, and the Φ_T values for the two compounds. These data are reported in Table 3. The measured Φ_T values of 0.20 (*cis* isomer) and 0.21 (*trans* isomer) closely resemble the values found for other members of the phthalocyanine and naphthalocyanine families.[6,8,9] That the intrinsic lifetime of the *trans* isomer T_1 state is only *ca.* 70% of that of the *cis* isomer gives a preliminary indication that the energy of the T_1 (*cis* isomer) is higher than that of the T_1 (*trans* isomer). This point is elaborated below.

Quenching by Oxygen. Under air-saturated conditions in benzene solution, the decay of the 640 nm absorbance of the

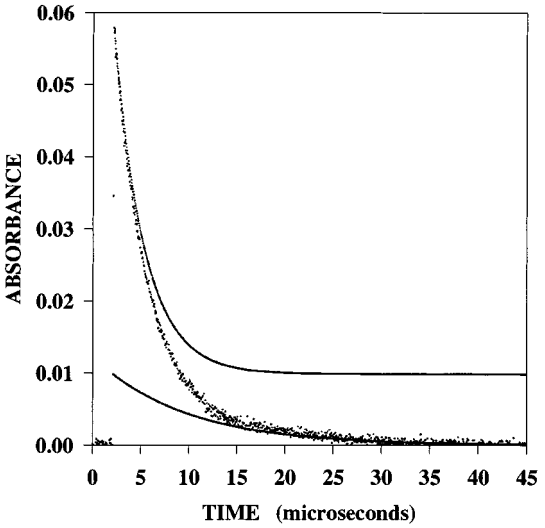

Figure 7. Time profile of the absorbance change at 640 nm following 355 nm laser excitation of an air-saturated solution in benzene of *cis* isomer (1.86 μM). The dots show the raw data points, and the full curves are the computer-fitted k_1 and k_2 components (see text).

Scheme 1

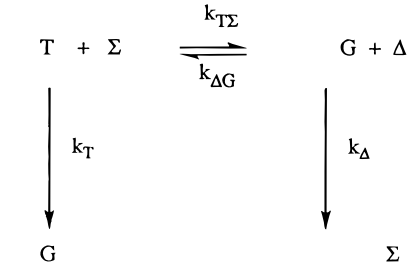

T_1 state of the *cis* isomer was enhanced over that in deaerated solution. However, the decay was nonexponential, being fitted best by a sum of two exponentials (Figure 7). The spectral properties at $t = 0$ μs and at $t = 15$ μs were identical, indicating that there were two kinetic pathways for the T_1 decay. This nonexponential behavior was maintained over a range of *cis* isomer concentration up to 16 μM. However, when the oxygen concentration was increased to values in excess of *ca.* 4 mM, the decay became single exponential. The *trans* isomer showed somewhat different behavior. Under air-saturated conditions, the decay was exponential over the whole range of chromophore concentration investigated (2−16 μM). At oxygen concentrations in excess of 3.7 mM, the decay of the triplet became nonexponential, similar to that observed for the *cis* isomer in air-saturated benzene solution.

Similar biphasic decay kinetics of T_1 states when quenched by oxygen have been observed previously for Pc and Nc derivatives[5,6] and were shown to be a consequence of the T_1 energy being close enough to that of singlet oxygen for the energy transfer step to be reversible under some applied conditions. A kinetic scheme (Scheme 1) was proposed where G and T represent ground and T_1 states of the photosensitizer respectively, Σ and Δ represent the $^3\Sigma^-_g$ and $^1\Delta_g$ states of molecular oxygen respectively, and $k_{T\Sigma}$, $k_{\Delta G}$, k_T, and k_Δ are the rate parameters for the reactions coupling the indicated species. In such cases involving reversible energy transfer where the rate of equilibration is faster than the reactions that drain the equilibrium, the time-variable triplet concentration $[T_1]$ can be fitted by the following general expression

$$[T_1]_t = A_1 e^{-k_1 t} + A_2 e^{-k_2 t} \quad (4)$$

where k_1 and k_2 are the observed fast and slow components of the triplet decay which are given by[5]

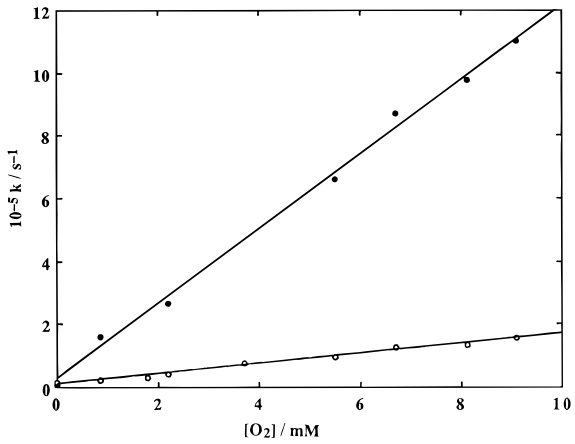

Figure 8. Variation with oxygen concentration of the early component (k_1) in the time profile (see Figure 7) of the triplet state decay of the isomers: (●) *cis* isomer (2 μM), (○) *trans* isomer (8 μM).

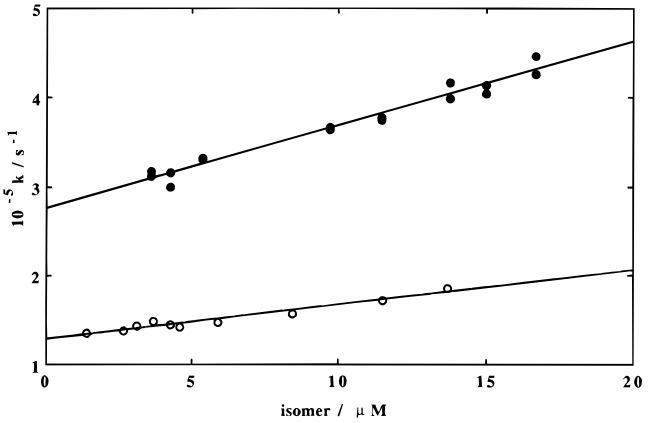

Figure 9. Variation of the rate constant for the early component (k_1) of the triplet decay of the isomers with isomer concentration: (●) *cis* isomer in air-saturated benzene solution, (○) *trans* isomer in air-saturated benzene solution.

$$k_1 = k_{\Delta G}[G] + k_{T\Sigma}[\Sigma] \quad (5)$$

and

$$k_2 = X_T k_T + X_\Delta k_D \quad (6)$$

where X_T and X_Δ are the mole fractions of the T and Δ species at equilibrium.

To verify that the present system is indeed described by such a kinetic model, the variations of k_1 with both O_2 and photosensitizer concentrations were evaluated independently. As shown in Figure 8, plots of the observed fast component (k_1) were linear with oxygen concentration with a slope $k_{T\Sigma} = 1.19 \times 10^8$ M^{-1} s^{-1} (*cis* isomer) and 1.6×10^7 M^{-1} s^{-1} (*trans* isomer). Moreover, plots of k_1 *vs* photosensitizer concentration (Figure 9) also show linear behavior, where values of $k_{\Delta G} = 0.93 \times 10^{10}$ M^{-1} s^{-1} (*cis* isomer) and 0.38×10^{10} M^{-1} s^{-1} (*trans* isomer) were extracted. From the intercepts, values of $k_{T\Sigma} = 1.25 \times 10^8$ M^{-1} s^{-1} (*cis* isomer) and 1.4×10^7 M^{-1} s^{-1} (*trans* isomer) were derived in excellent agreement with those extracted from the variance of k_1 with [O_2]. The linearity of the plots in Figures 8 and 9 serves to indicate that the kinetic analysis based on Scheme 1 properly describes the situation. On the basis of these reverse and forward rate constants, the equilibrium constant K_e ($=k_{T\Sigma}/k_{\Delta G}$) was calculated to be 0.013 for the *cis* isomer and 0.0037 for the *trans* isomer.

Alternatively, K_e may be obtained from the values of the absorbances of T_1 at $t = 0$ (A_o) and at equilibrium (A_∞):

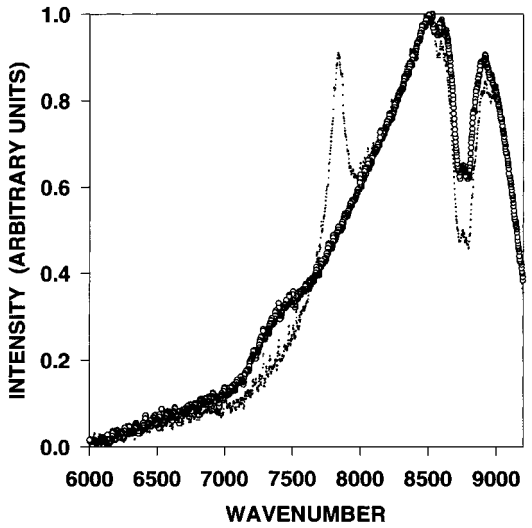

Figure 10. Phosphorescence spectra of *cis* isomer (11.2 μM) in benzene at room temperature: O_2-saturated solution (●) and N_2-saturated solution (○). The spectra have been normalized at 8400 cm^{-1}.

$$K_e = ([G]/[\Sigma])/\{(A_o - A_\infty)/A_o\} \quad (7)$$

In this case, A_o and A_∞ were obtained from experimental traces such as that in Figure 7. Values of K_e obtained by this method using *cis* isomer concentrations in the range of 3−15 μM in air-saturated benzene solutions yielded an average value of 0.011, close to the value obtained from the rate constant data. For the same experiments employing the *trans* isomer (up to *ca* 5 μM), a value of $K_e = 0.004$ resulted, again in line with the value obtained from kinetic experiments. Thus, the reversible energy transfer to oxygen and the less-than-unity equilibrium constants point to the fact that the T_1 energies of the *cis* and *trans* isomers are below that of singlet oxygen. The observed differences between the decay kinetics of the two triplet states in air-saturated benzene arise from the different values of K_e which characterize the reversible energy transfer (Scheme 1). The absolute magnitude of K_e determines the oxygen concentration conditions under which single-exponential kinetics occur.

From the equilibrium constant values derived here, it is possible to estimate the triplet state energies, since K_e is related to the difference in energy between the T_1 state in question and the known energy of singlet oxygen. Equation 8 expresses this relationship

$$RT \ln K_e = E_T - E_\Delta + RT \ln(^1/_9) \quad (8)$$

where E_Δ is the energy of the $^1\Delta_g$ state of oxygen and the factor $^1/_9$ is a spin-statistical parameter which arises from the fact that in the T_1-O_2 collision only one-ninth of the encounter complexes can proceed to overall singlet products. Thus, the equilibrium-derived value of E_T is depressed from the true spectroscopic value.

For the *cis* isomer, Table 3 yields $K_e = 0.013$, which for $E_\Delta = 22.5$ kcal mol^{-1}, eq 8 yields a value of $E_T = 22.5-1.25 = 21.2$ kcal mol^{-1}. Similarly, E_T (*trans*) = 20.52 kcal mol^{-1}. Thus, energy transfer from the *cis* isomer to oxygen is 1.25 kcal mol^{-1} endoergic, while that from *trans* is 2.0 kcal mol^{-1} endoergic.

The triplet energies of chromophores can also be obtained in principle from phosphorescence spectra of the compounds in question. To this end, spectral studies were conducted of the near-infrared luminescence from the *cis* and *trans* isomers in N_2- and O_2-saturated benzene solutions at room temperature (Figure 10). For the *cis* isomer, a band was observed in N_2-

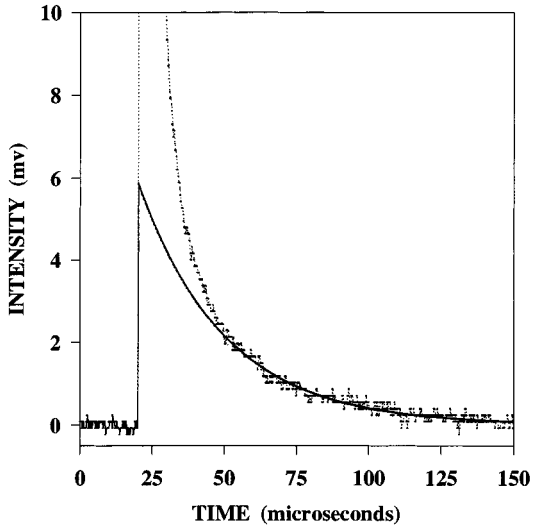

Figure 11. Time profile of the near-infrared luminescence intensity after 355 nm laser excitation of an air-saturated benzene solution of *cis* isomer (13 μM) in benzene.

saturated benzene solution with a maximum centered at 7400 cm^{-1} (1350 nm), which converts to a value of $E_T = 21.2$ kcal mol^{-1}, identical within the error margin of that determined from the equilibrium kinetics experiment using eq 7. This phosphorescence band disappeared upon oxygen saturation, to be replaced by a new band at 7800 cm^{-1} (1282 nm), arising from the radiative transition $^1\Delta_g \rightarrow {}^3\Sigma^-_g$ transition in O_2. A different behavior was observed for the *trans* isomer. In N_2-saturated solutions, it was not possible to definitively identify any feature that could be assigned to a phosphorescence signal. Upon oxygen saturation, a weak luminescence at 7800 cm^{-1} appeared, indicating that singlet oxygen was being formed.

Singlet Oxygen Production. Air-saturated solutions of both the *cis* and *trans* isomers in benzene emitted luminescence in the near-infrared near 1.27 μm upon excitation by 10 ns pulses of 335 nm light. Figure 11 shows a typical emission profile. As outlined in the Experimental Section, the slow component is the emission from singlet oxygen formed by energy transfer from the triplet photosensitizer to ground state molecular oxygen. A plot of $L_0(x)$ *vs* L_0(r) for the *cis* isomer is shown in Figure 12. From the slope of this plot, a value of $\Phi_\Delta = 0.20 \pm 0.04$ was derived. Employing a similar procedure for the *trans* isomer (data not shown) provided a value of $\Phi_\Delta = 0.18 \pm 0.04$. All photophysical properties of the *cis* and *trans* compounds are summarized in Table 3.

Thus, like the octabutoxyphthalocyanines and naphthalocyanines that have been synthesized and photophysically characterized in these laboratories, the *cis*- and *trans*-dibenzophthalocyanines have triplet states with energies close to that of singlet oxygen such that reversible electron exchange energy transfer is facile. Like these same compounds, the deep-red absorptions and significant singlet oxygen quantum yields should make the title compounds effective as deep-red PDT agents and in optical recording.

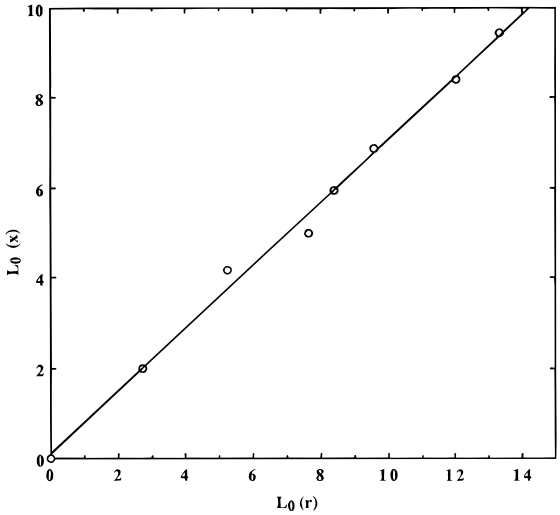

Figure 12. Plot of L_0(x) vs L_0(r) (see text) for an air-saturated benzene solution of *cis* isomer (13 μM).

Conclusions

The new route to silicon-centered phthalocyanines and phthalocyanine-like compounds developed in the course of this study is robust and flexible and thus of considerable potential usefulness. Examination of the positions of the Q-bands of the 18 metal-free, dihdroxysilicon and bis-trihexylsiloxysilicon octabutoxy- and octabutoxybenzophthalocyanines made in the study shows that these bands appear at understandable wavelengths. The wavelength of the Q-band of *c*-$SiN_2P_2(OBu)_8(OSi(n\text{-}C_6H_{13})_3)_2$ (804 nm) is of potential clinical and technological importance because it matches the wavelength of the output of the most common GaAlAs diode laser. On the basis of the wavelengths of the Q-bands of the compounds made in this study and those of phthalocyanine and phthalocyanine-like compounds made in other studies, it is clear that it is possible to tailor such compounds to have Q-bands with any of a wide range of wavelengths.

The ^{1}H and ^{13}C NMR resonances of the 18 compounds, like their Q-bands, appear in understandable positions.

The isomeric pair of compounds *c*- and *t*-$SiN_2P_2(OBu)_8(OSi(n\text{-}C_6H_{13})_3)_2$ have no tendency to aggregate in benzene in the range of concentrations up to 150 μM. Laser flash photolysis studies indicate that the absorption maximum of the triplet state of the *cis* isomer is at 640 nm and its lifetime in deaerated benzene is 105 μs and that the maximum of the triplet of the *trans* isomer is at 660 nm and its lifetime is 72 μs. Both isomers have triplet quantum yields of *ca*. 0.20 and singlet oxygen quantum yields of *ca*. 0.20, photophysical properties that are consistent with efficient photosensitization action in the photodynamic therapy of tumors.

Acknowledgment. The work was supported in part by NIH grants CA 46281 and GM 24235 and by the Center for Photochemical Sciences at Bowling Green State University.

JA963702Q